BAY AREA AIR QUALITY MANAGEMENT DISTRICT
939 Ellis Street, San Francisco, CA 94109

Research and Modeling Section Publication No. 201003-005-PM-O3

Characterization of Inter-basin PM and Ozone Transport for the Bay Area

March, 2010

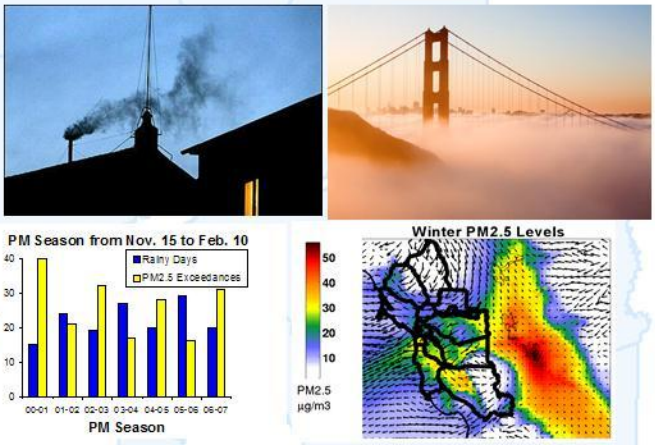

Prepared by:
Ahmet Palazoglu, Professor
Department of Chemical Engineering and Materials Science
University of California at Davis

Contributors:
Angadh Singh, UC Davis
Scott Beaver, BAAQMD

Prepared for:
Saffet Tanrikulu, Manager, Research and Modeling Section

Table of contents

Table of figures

Table of tables

Executive summary

E.1 Description of study

This study investigated weather patterns under which wintertime fine particulate matter ($PM_{2.5}$), summertime ozone, and their precursors may be transported between the San Francisco Bay Area (SFBA), and the Sacramento area and the San Joaquin Valley (SJV). However, the study did not confirm the presence of transport or quantify it. The transport assessment can be made by simulating air quality with the identified weather patterns using photochemical models or any other tools available.

The study applied a state-of-the-science data mining technique to identify representative weather patterns. Transport of $PM_{2.5}$ was analyzed for the winter months (November-March), and transport of ozone was analyzed for the summer months (May-October). The analysis included most days from a 9-year historical record (1999-2007). This large sample size ensured robust identification and characterization of all historically important $PM_{2.5}$ and ozone transport pathways impacting Central California attainment status for these regional pollutants.

This study identified and labeled the times of occurrence for representative weather patterns controlling $PM_{2.5}$, ozone, and precursor buildup around the SFBA and surrounding regions. Atmospheric processes impacting $PM_{2.5}$ and ozone buildup were then inferred to the extent possible using available measurements. These inferences allowed qualitative ranking of the identified weather patterns in terms of their transport potentials. The overall goal of the study was to identify representative weather patterns having the potential for significant to overwhelming levels of transported pollutants between districts. Frequencies of occurrence for such “transport patterns” were tabulated. These frequencies reflected the average number of exceedance days per year associated with each identified transport pattern.

The primary project deliverables were recommendations for future research to quantify the impacts of the various transport patterns identified qualitatively in this study. (These recommendations are outlined in section E.4.) Ultimately, the results of this study will guide future BAAQMD modeling and field study efforts to accurately quantify year-round SFBA transport impacts for $PM_{2.5}$ and ozone. This relatively low-cost and broad-based study provides the underpinning for future $PM_{2.5}$ and ozone transport analyses that will require increasingly costly and specific research projects. Without the guidance provided by this study, more detailed and quantitative transport studies would be highly unlikely to provide representative and accurate findings.

E.2 Winter PM results

Transport of $PM_{2.5}$ and precursors during the winter season tended to occur mostly from the Central Valley into the SFBA. Two different episodic transport patterns were

identified. The first transport pattern accounted for around 60% of all SFBA 24-hr $PM_{2.5}$ exceedances. $PM_{2.5}$ and precursors were likely transported mostly from the Sacramento area through Carquinez Strait. The second transport pattern accounted for around 20% of all SFBA 24-hr $PM_{2.5}$ exceedances. $PM_{2.5}$ and precursors were likely transported mostly from the SJV through Carquinez Strait and also Altamont Pass.

E.2.1 Transport pattern from the Sacramento area

The weather pattern with transport mostly from the Sacramento area was persistent. It occurred when an aloft ridge of high pressure was positioned over Central California. Conditions throughout Central California were near calm, stable, and subsiding. Capping thermal inversions often formed at low levels. This three-dimensional structure of the lower atmosphere inhibited vertical dispersion of pollutants away from the surface. The surface air flows were decoupled from the aloft winds. Light, shallow terrain induced air flows developed throughout Central California.

In the Central Valley, persistent drainage (downslope) flows developed over its slopes. These flows converged toward the Central Valley floor, increasing low-level atmospheric pressure. These winds then emptied through Carquinez Strait, the only major gap in the Central Valley rims, and passed through the SFBA. A downvalley flow developed in the Sacramento Valley (SV) along its major axis. The flow pattern was directed through Sacramento and toward the Delta region. This downvalley flow was connected to the winds entering the SFBA through Carquinez Strait.

Considerable transport of $PM_{2.5}$ and precursors was likely to have occurred from the Sacramento area. Transported wood burning $PM_{2.5}$ may play a major role in contributing to SFBA PM. Regionally accumulated pollutants from around the Delta region may have also been transported into the SFBA. Under this weather pattern, transport from the northern SJV into the SFBA was also possible through Altamont Pass. SFBA $PM_{2.5}$ levels were regionally elevated and somewhat higher at San Jose than for the other monitoring locations. In the SJV, conditions were relatively calm. Ammonium nitrate formed rapidly upon the reaction of available nitric acid with the SJV ammonia emissions, especially from its concentrated dairying operations. Ammonium nitrate accumulated regionally to high levels throughout the SJV during this weather pattern. This weather pattern could persist for up to weeks. It often resulted in very high $PM_{2.5}$ levels throughout Central California and multi-day exceedance periods for the SFBA.

E.2.2 Transport pattern from the San Joaquin Valley

The weather pattern with transport mostly from the SJV area was transient. It typically lasted for at most a few days. When it occurred, it almost always immediately followed the above (E.2.1) described episodic conditions with transport mostly from the Sacramento area. Transport from the SJV was usually followed by strong, southerly (from the south) winds driven through the complex Central California terrain by the counterclockwise motions of an approaching offshore low pressure cell (storm). The $PM_{2.5}$ that had previously accumulated in the SJV, mostly ammonium nitrate, was

transported to the north by this southerly flow. Transport from SJV occurred into both the SFBA and the SV. Winds were strong and vertical dispersion was increasing; however, the previously accumulated SJV pollutants were transported considerable distances northward before the plume was dispersed. The plume of transported $PM_{2.5}$ usually affected the eastern and northern portions of the SFBA only. San Jose was mostly unaffected. It occurred less frequently than the above pattern with transport mostly from the Sacramento area. It was, however, likely associated with higher levels of transported $PM_{2.5}$. In one extreme case (7 January 2001), this transport pattern appears to have triggered an East Bay 24-hr $PM_{2.5}$ exceedance (35 $\mu g/m^3$) that would have occurred in the absence of any SFBA emissions. This transient transport pattern was always followed by unstable, stormy conditions in which accumulated pollutants were rapidly scoured away from the Central California surface.

E.2.3 Local pattern

Winter weather patterns were observed having marine winds entering the SFBA from the west. Winds entered the SFBA, passed through Carquinez Strait, and then flowed into the Central Valley. These weather patterns were unlikely to have been associated with significant levels of transport. Strong vertical dispersion and high wind speeds produced adequate ventilation of the surface. $PM_{2.5}$ and precursor levels were generally low because pollutants were dispersed upward before they could be appreciably advected horizontally. Little transport at low levels was likely to have occurred from the SFBA into the Central Valley.

E.3 Summer ozone results

Two different types of ozone episodes were identified in Central California. One of them occurred mid-summer (mid-June through late August) and the other occurred late summer (late August through mid-October).

E.3.1 Transport pattern for mid-summer

Mid-summer ozone episodes mostly developed under an onshore high pressure system (an aloft anticyclone) in Central California. Under this condition, the large-scale pressure gradient was weak and a localized sea breeze developed between cool coastal locations and hot inland locations. This localized flow was shallow, and vertical dispersion of ozone and its precursors was inhibited. Pollutants were transported from the SFBA, through Carquinez Strait, and into the Central Valley.

The anticyclone was a semi-permanent mid-summer feature; however, its strength and spatial extent varied considerably. Two weather patterns were identified in which the anticyclone had expanded over Central California. In both cases, the strength of the anticyclone impacted wind speed. When the anticyclone was very strong, the sea breeze extended mostly into the northern SJV. In the central and southern SJV, wind speed was relatively low. Because of relatively slow winds, it is unlikely that SFBA morning emissions reached the central SJV on or before ozone exceedances occurred. When the anticyclonic pattern was diminished in strength, large-scale marine winds were

superimposed on the sea breeze flow pattern. This resulted in high wind speeds through Carquinez Strait. Flows through Carquinez Strait split into both the SV and the SJV. Relative to the more strongly anticyclonic transport pattern, this less strongly anticyclonic transport pattern ventilated the Delta region as well as much of the SJV. Pollutants were transported beyond the Delta, deeper into the Central Valley. However, ozone exceedances were rare for this relatively ventilated transport pattern.

E.3.2 Transport pattern for late summer

Late summer ozone episodes mostly developed under an offshore high pressure system (an aloft ridge). During these ridging conditions, little flow occurred through Carquinez Strait. Sea breeze was weak because of diminished temperature differential between coastal and inland locations. The SFBA was largely decoupled from the Central Valley. Conditions leading into these episodes were typically well ventilated and ozone levels were relatively low. As the offshore ridge approached California from the west, strong winds entered the SV from the north and flowed into the SJV. Ozone levels were moderate under the strong winds; however, ozone and precursors may have been transported from the Sacramento area into the SJV and occasionally into the SFBA. Conditions became near-stagnant throughout Central California as the ridge moved over the shoreline. This weather pattern resulted in many of the highest ozone levels recorded for Central California. Transport from the SFBA during these episodes was unlikely. Also, because these episodes were typically preceded by well ventilated conditions, they were unlikely to have been driven by previously transported SFBA pollutants. This weather pattern reflected conditions in which Central Valley ozone episodes were not likely to have been impacted by SFBA emissions.

E.4 Recommendations

This study identified a variety of weather patterns under which transport may have been likely to occur. This measurements-based study, however, can neither confirm the presence of transport nor quantify it. The next step in a comprehensive transport assessment is to simulate the identified transport patterns using photochemical models. We strongly recommend a seasonal photochemical modeling approach in which entire winter and summer seasons are simulated. This seasonal approach is likely the most practical framework through which representative occurrences of all transport patterns can be simulated. Additionally, simulations may be useful to confirm the lack of significant transport suspected for certain weather patterns. Multiple winter and summer seasons should be selected to ensure that representative occurrences of major transport patterns of interest are explored. The seasons selected for modeling should also have representative numbers of exceedance days.

Winter photochemical modeling should simulate the two different types of identified transport patterns. The pattern with transport mostly from the Sacramento area occurred frequently during most winters. The other pattern with transport mostly from the SJV, however, occurred far less frequently. Also, the level of transport associated

with this latter pattern was in some cases extreme. Therefore, the representative occurrences of this latter type of transport pattern (transport mostly from the SJV) should be a primary consideration when selecting winter seasons for modeling. The simulations should be conducted to confirm the lack of significant transport from the SFBA into the Central Valley under conditions having marine flows from the west.

Summer photochemical modeling should simulate the two different types of ozone episodes identified. Mid-summer episodes occurring under onshore high pressure systems should be simulated with strong, moderate, and weak large-scale marine flows superimposed on localized sea breeze flows. Such modeling may be able to distinguish differences in the level and distance for transport resulting from different flow strengths and depths through the SFBA. Late summer episodes occurring under an offshore ridge of high pressure should also be simulated to confirm a lack of significant transport from the SFBA into the Central Valley.

Photochemical modeling is the best available tool to quantify transport impacts. Robust and accurate transport impact estimates can be obtained by pooling the model results across the days identified by this study that share common transport patterns. Ideally, these photochemical modeling results should be validated against tracer field studies to confirm the modeled source-receptor relationships.

Characterization of Inter-basin PM and Ozone Transport for the Bay Area

1. Introduction

1.1 Overview of study

The San Francisco Bay Area (SFBA), the San Joaquin Valley (SJV), and the Sacramento area within the Sacramento Valley (SV) have been designated as federal nonattainment areas for both ozone and fine particulate matter ($PM_{2.5}$). These major Central California air basins are connected at the Delta region, where they may exchange air flows. Emissions of pollutants and their precursors in each of these interconnected basins contribute to regional buildup of ozone and $PM_{2.5}$. Unhealthy air pollution levels result from some combination of locally emitted and transported pollutants. The transport impacts likely vary from day to day with the prevailing weather. The purpose of this study was to identify representative airflow patterns for potential transport of ozone and $PM_{2.5}$ in the region. The study emphasized patterns providing potential transport into and from the SFBA.

1.2 Background

Since 1989, the California Health and Safety Code (§ 39610) has charged the Air Resources Board (ARB) to study the effects of air pollutants transported from upwind air basins into downwind air basins. This inter-basin transport analysis is to be reviewed and updated every three years with such precision necessary to determine whether the effects of pollutants transported between basins are *overwhelming*, *significant*, *inconsequential*, or *some combination* of these three categories.

Typically, *surface wind field analyses* and *wind trajectory calculations* have been used to assess pollutant transport qualitatively. These methods are indeed capable of determining source areas that are upwind of downwind receptor areas; however, such simple relationships are not highly relevant to pollutant transport assessment. Surface wind fields and wind trajectories do not account for the three-dimensional physical and chemical processes affecting ambient pollution. Pollutants emitted from an upwind source may well be dispersed, deposited to surfaces, and/or chemically transformed by the time the air mass reaches the downwind receptor.

Photochemical modeling does simulate three-dimensional physics and chemistry and has been applied for transport assessment. Photochemical models are, however, extremely resource intensive. Thus, photochemical modeling for Central California transport assessment has only been applied to a few (subjectively selected) relatively brief pollution episodes. Such an “episodic modeling” approach cannot possibly

accurately estimate representative, real-world transport impacts that are likely to occur in the future.

1.3 Transport analysis framework

Ultimately, photochemical modeling is the best available tool to quantitatively assess the transport impacts. But, extensive simulation of all possible conditions under which transport may have occurred is impractical. A practical approach is to first identify all weather patterns under which transport may have occurred. Then, estimate transport impacts, using photochemical models, for representative occurrences of each identified weather pattern. Overall transport impacts can be expressed as a weighted sum of the individual impacts for each weather pattern. The weights correspond to the relative frequencies of occurrence for the weather patterns. This is the most efficient framework by which transport impacts can be robustly assessed.

This study applied the first systematic and rigorous analysis of weather patterns impacting pollutant transport around the SFBA and surrounding regions. A state-of-the-science *data mining technique* was used to identify representative weather patterns under which transport may have occurred. The data mining technique directly identified air flow patterns that exhibited the potential for pollutant transport. It also identified real weather patterns and allowed inferences of the contributions of their relevant three-dimensional atmospheric processes impacting pollutant transport. This conceptual understanding helped rank the weather patterns in terms of their likelihoods for transport to have occurred.

The results of this study will feed into future BAAQMD photochemical modeling efforts in the selection of representative transport events to simulate. Robust, quantitative transport impacts estimates will then be obtained using the framework outlined above.

1.4 Study goals

There were four major goals of this study.

1. Identify and label the times of occurrence for representative weather patterns controlling ozone, $PM_{2.5}$, and precursor buildup around the SFBA and surrounding regions.
2. Characterize the atmospheric processes driving ozone and $PM_{2.5}$ buildup under each identified weather pattern.
3. Infer the role that transport may have played in pollutant buildup around key Central California monitoring locations. Rank the weather patterns in terms of their inferred transport potential.
4. Recommend representative transport patterns for photochemical modeling. Provide frequencies of occurrence for the transport patterns to allow estimation of overall, cumulative transport impacts from the simulations of representative events.

2. Methods

2.1 Algorithms applied

The primary methods used in this study are data mining techniques known as *cluster analysis* and *sequence analysis*. The state-of-the-science clustering (Beaver and Palazoglu, 2006) and sequencing (Beaver et. al., 2008) algorithms have been applied. The clustering technique identifies groups of days, or *clusters*, sharing similar average meteorological conditions. The clusters are real, three-dimensional weather patterns reflecting atmospheric processes controlling pollutant buildup. The atmospheric processes associated with each weather pattern are determined by averaging available measurements across the days assigned to that pattern. Characterization of these atmospheric processes allows inference of pollutant buildup mechanisms, including potential transport impacts.

The clustering method requires several years of continuous, high quality hourly surface wind measurements covering the study domain of interest. Periods having missing or biased measurements must be excluded from the clustering. A statistically imputing method can be used for filling any short gaps in the data of less than 6 hours (Schneider, 2001). In practice, surface monitoring locations providing inputs to the algorithm must be judiciously selected to balance spatial coverage and temporal continuity. After the clustering has been performed, it is often possible to classify days having partially missing data into the weather patterns identified by the clustering.

The sequencing technique identifies multi-day periods, or *scenarios*, sharing similar day-to-day evolutions of the meteorological conditions. These scenarios represent different types of idealized air pollution episodes that develop, possibly persist, and then dissipate. The scenarios are defined in terms of *atmospheric transitions* between two different weather patterns (clusters) that occur over consecutive days. A *favored* atmospheric transition reflects the natural tendency for one specific weather pattern to lead into another specific weather pattern. Transitions that are favored at higher levels of significance (smaller values of α) tend to occur at higher relative frequencies.

2.2 Transport analysis

For this study, the methods were applied primarily to estimate transport impacts involving the SFBA. Most transport was believed to have occurred between the SFBA and the Central Valley. Therefore, the methods were applied to input data spanning both SFBA and Central Valley locations.

Separate cluster analyses were applied to analyze transport impacts for winter $PM_{2.5}$ and summer ozone. This pair of seasons tended to exhibit air flow patterns in opposite directions, implying very different transport characteristics. During the winter months, most transport was believed to have occurred into the SFBA. Identification of these transport patterns required cluster analysis of measurements from the Bay Area as well

as from the Delta region immediately upwind of the SFBA. During the summer months, most transport was believed to have occurred from the SFBA. Flow splitting of the winds passing through the SFBA and into the Central Valley may have occurred around the Delta region. Identification of these transport patterns required cluster analysis of measurements from the bay Area, the Delta region, the southern SV, and the northern SJV. Additional information on the data sets used for clustering is given in section 3.

Separate sequence analyses were applied to characterize winter $PM_{2.5}$ episodes and summer ozone episodes. The sequencing characterized the timing between emissions, ambient pollutant buildup, and subsequent transport. In some cases, pollutant buildup may have occurred for a region under a given weather pattern. However, transport of the accumulated pollutants may have occurred under a different (subsequent) weather pattern.

2.3 Transport inferences

Inferences of transport impacts were made for each weather pattern based on the average atmospheric processes associated with that pattern. The methods applied in this study allowed inferences of the *potential* for the identified weather patterns to exhibit pollutant transport. Actual occurrences of transport can only be proven through a combination of photochemical modeling and tracer field studies.

All inferences drawn in this study were based on analysis of average meteorological and air quality patterns. In reality, however, each analyzed day was unique and may be somewhat different than the averaged fields. Furthermore, some data were missing for certain parameters on certain days resulting in the use of subset of data in characterizing the atmospheric processes. For these reasons, the inferences drawn for the weather patterns may not strictly apply to every day assigned to that weather pattern. However, the large sample sizes used in this study minimized the uncertainty due to the above reasons. In aggregate, the patterns discussed in this report are believed to be reasonably representative, accurate, and physically meaningful. They provided meaningful insights to the dominant atmospheric processes associated with the average impacts of pollutant buildup, dispersion, and transport.

3. Data

3.1 Data sources and processing

Data for this study were obtained from multiple sources. Surface meteorological and air quality measurements were obtained for the locations shown in Figure 1. Surface meteorological measurements for weather stations located within SFBA were provided by the Bay Area Air Quality Management District (BAAQMD). Oakland sounding measurements were also provided by the BAAQMD. Central Valley meteorological data were obtained from the California Air Resources Board (CARB). All air quality data ($PM_{2.5}$, ozone, and NO_x levels) were obtained from the CARB 2009 Air Quality Data DVD. Weather maps were obtained from NCEP/NCAR Reanalysis (http://www.cdc.noaa.gov).

All data were processed for compatibility with software developed previously at the Palazoglu Lab at UC Davis. High quality wind measurements were critical to the successful identification of potential transport patterns. Therefore, all wind measurements from weather stations used in the clustering were rigorously screened for correctness using the procedure described in Beaver and Palazoglu (2008).

3.2 Winter data

In total, 13 weather stations provided the wind measurements used as inputs to the winter cluster analysis (Table 1). These stations were selected to sample flows around and also immediately upwind of the SFBA during winter episodic conditions. There were 8 stations within the SFBA. Another 5 stations were located between the northern SJV and Sacramento area. Availability of measurements from these locations is shown in Figure 2. The clustered data spanned 8 winter PM seasons from 1999-2007.

The SFBA wind measurements were of high quality. Wind data for most sites in the Central Valley, however, were prone to biased and inconsistent measurements. Many low quality Central Valley wind data were removed from the data sets for the purpose of analysis.

Hourly temperature measurements were obtained for Fort Funston, Concord, Modesto, and Davis. Daily cumulative precipitation data were obtained from Concord, Sacramento, and Modesto.

Daily (24-hr averaged) FRM (federal reference method) gravimetric total $PM_{2.5}$ measurements were obtained for 15 locations around the SFBA and Central Valley (Table 2). Co-located BAM measurements for total 24-hr averaged $PM_{2.5}$ were available for a subset of these locations (not shown). Speciated 24-hr averaged $PM_{2.5}$ measurements were obtained for San Jose-Jackson Street in the SFBA, Modesto-14th Street in the northern SJV, and Sacramento-Del Paso Manor in the SV. The speciated

measurements were performed every 6th day. Most $PM_{2.5}$ monitors operated for most of the study period, but operating schedules varied by location.

3.3 Summer data

In total, 21 weather stations provided the wind measurements used as inputs to the summer cluster analysis (Table 3). These stations were selected to sample flows around and also considerable distances downwind of the SFBA during summer episodic conditions. There were 8 stations within the SFBA. Another 13 stations were located between the central SJV and the central SV. Availability of measurements from these locations is shown in Figure 3. The clustered data spanned 8 summer ozone seasons from 2000-2007.

The SFBA wind measurements were of high quality. Wind data for most sites in the Central Valley, however, were prone to biased and inconsistent measurements. Many low quality Central Valley wind data were removed from the data sets for the purpose of analysis.

Hourly temperature measurements were obtained for 22 locations throughout Central California.

Daily 8-hr averaged ozone measurements were obtained for 31 locations throughout Central California (Table 4). Hourly NO_x (NO and NO_2) measurements were available for most of these air quality monitoring locations. Most of the air quality monitors operated for the duration of the study period.

Table 1. Names, BAAQMD codes, and positions for 13 surface weather stations used for winter transport clustering. All stations recorded hourly wind speed and direction.

Site Name	Site ID	Latitude	Longitude	Elevation (m)
Bethel Island	2901	37.95	-121.70	-1.5
Concord	2903	37.94	-122.03	23.6
Fort Funston	5905	37.72	-122.50	57.0
Kregor Peak	2905	37.94	-121.90	577.4
Pt. San Pablo	2907	37.96	-122.42	70.1
Pleasanton STP	1905	37.70	-121.93	99.1
San Martin APT	7901	37.09	-121.60	85.3
Suisun STP	8801	38.23	-122.07	5.3
Modesto-14th Street	2833	37.64	-120.99	N/A
Stockton-Hazelton	2094	37.95	-121.27	N/A
Rio Vista	8901	38.19	-121.71	10.7
Davis-UCD Campus	2143	38.53	-121.77	N/A
Roseville-N Sunrise Blvd	2956	38.75	-121.26	N/A

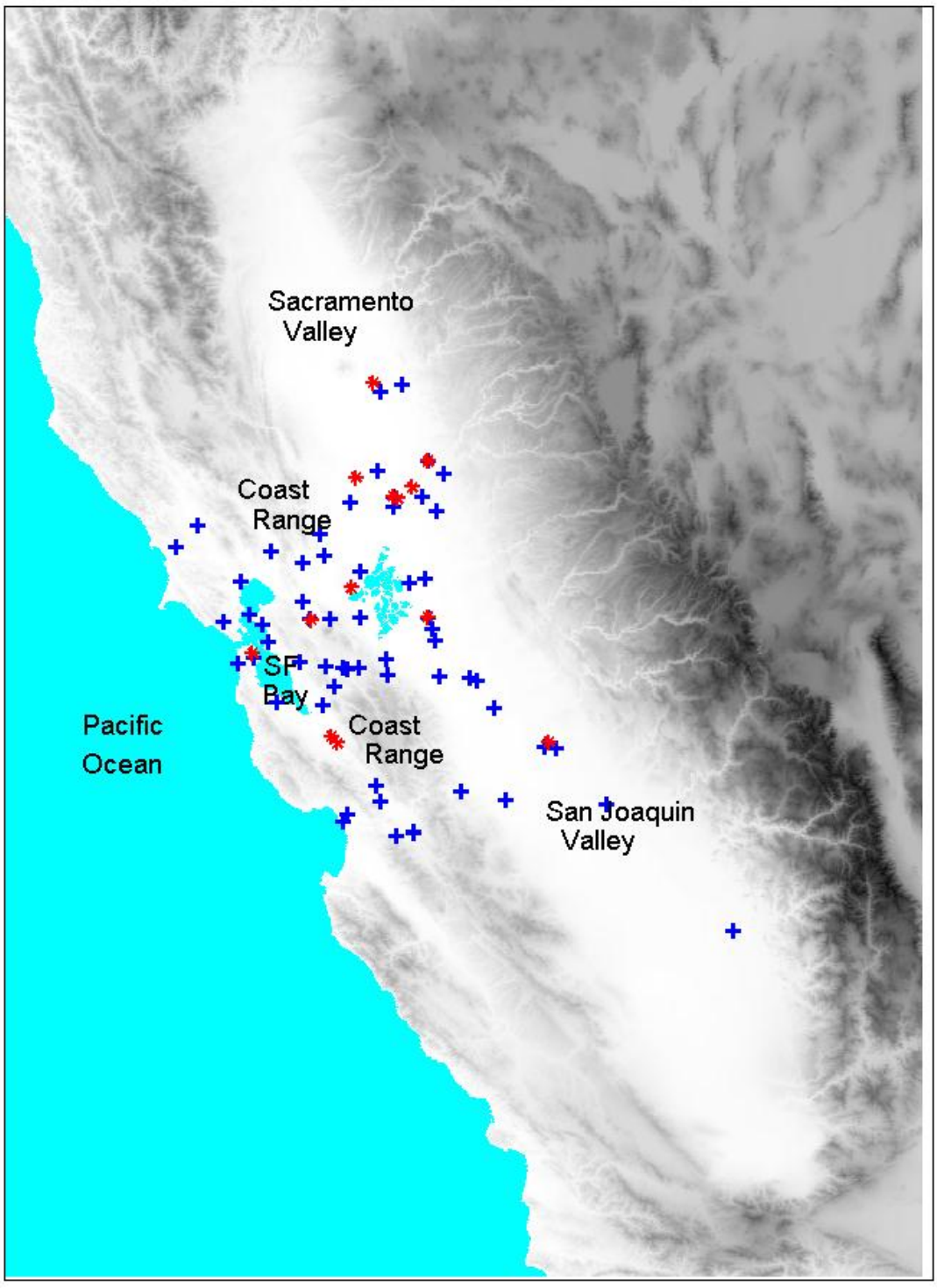

Figure 1. Map of study domain comprising SFBA, SJV, and SV. Locations of surface weather stations (blue +) and air quality monitors (red *) are indicated.

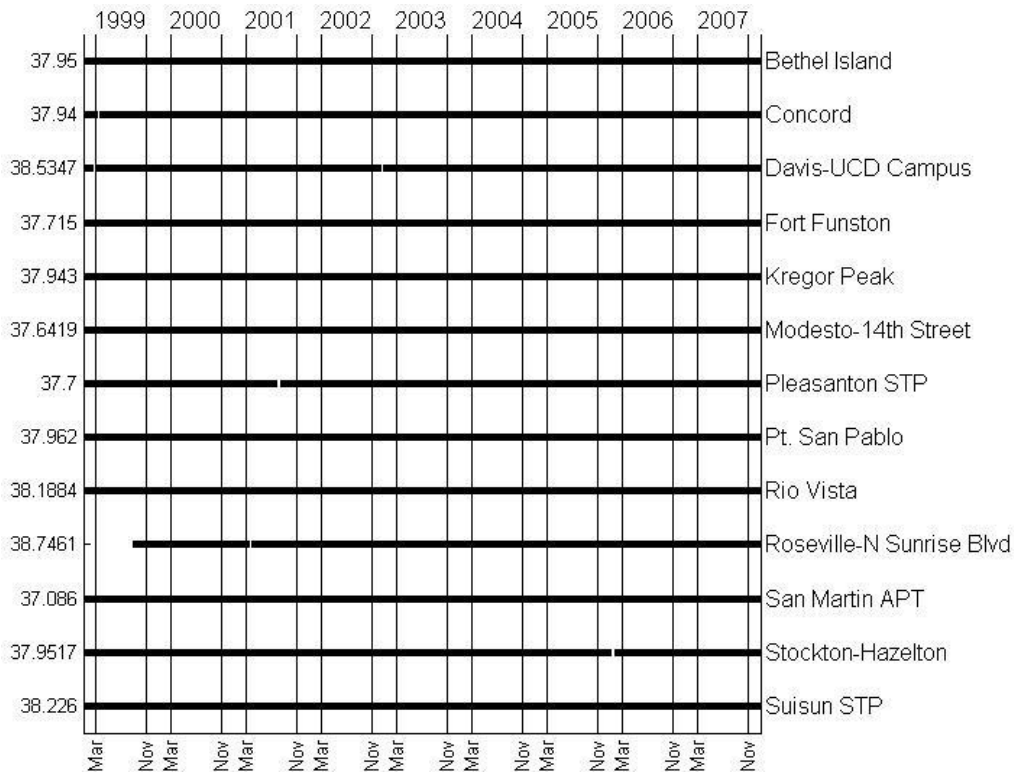

Figure 2. Availability of wind data from weather stations used in the winter transport clustering. Solid horizontal lines indicate periods for which wind data are available for a given station. Vertical lines appear at 1 November and 31 March. Years centered over summer months along top.

Table 2. Names, CARB site codes, and positions for 15 $PM_{2.5}$ monitors.

Site Name	Site ID	Latitude	Longitude	Tower height (m)
Stockton-Hazelton Street	2094	37.95	-121.27	10
Sacramento-Health Dept Stockton Blvd	2346	38.56	-121.46	10
San Francisco-Arkansas Street	2373	37.77	-122.40	10
Vallejo-304 Tuolumne Street	2410	38.10	-121.76	10
San Jose-4th Street	2413	37.34	-121.89	10
Sacramento-Del Paso Manor	2731	38.61	-121.37	10
Concord-2975 Treat Blvd	2831	37.94	-122.02	10
Modesto-14th Street	2833	37.64	-120.99	10
San Jose-Tully Road	2936	37.31	-121.85	10
Roseville-N Sunrise Blvd	2956	38.74	-121.26	10
Yuba City-Almond Street	2958	39.14	-121.62	10
Sacramento-T Street	3011	38.57	-121.49	10
Woodland-Gibson Road	3249	38.66	-121.73	10
Merced-2334 M Street	3253	37.31	-120.48	10
Livermore-793 Rincon Avenue	3490	37.69	-121.78	10

Table 3. Names, CARB site codes, and positions for 21 surface weather stations used for summer transport clustering. All stations recorded hourly wind speed and direction.

Site Name	Site id	Latitude	Longitude	Elevation (m)
Bethel Island	2901	37.95	-121.70	-1.5
Concord	2903	37.94	-122.03	23.6
Fort Funston	5905	37.71	-122.50	57.0
Kregor Peak	2905	37.94	-121.90	577.4
Pt. San Pablo	2907	37.96	-122.42	70.1
Pleasanton STP	1905	37.70	-121.93	99.1
San Martin APT	7901	37.09	-121.60	85.3
Suisun STP	8801	38.22	-122.07	5.3
Modesto-14th Street	2833	37.64	-120.99	N/A
Stockton-Hazelton	2094	37.95	-121.27	N/A
Manteca	N/A	37.84	-121.22	N/A
Rio Vista	8901	38.19	-121.71	10.7
Davis-UCD Campus	2143	38.53	-121.77	N/A
Roseville-N Sunrise Blvd	2956	38.75	-121.26	N/A
Visalia-N Church Street	2032	36.33	-119.29	N/A
Colusa #2	5720	39.23	-122.02	N/A
Gerber	5712	40.05	-122.16	N/A
Gridley-Cowee Avenue	2630	39.33	-121.67	N/A
Kesterson	5752	37.03	-120.88	N/A
Parlier #2	5723	36.60	-119.50	N/A
Winters	5784	38.50	-121.97	N/A

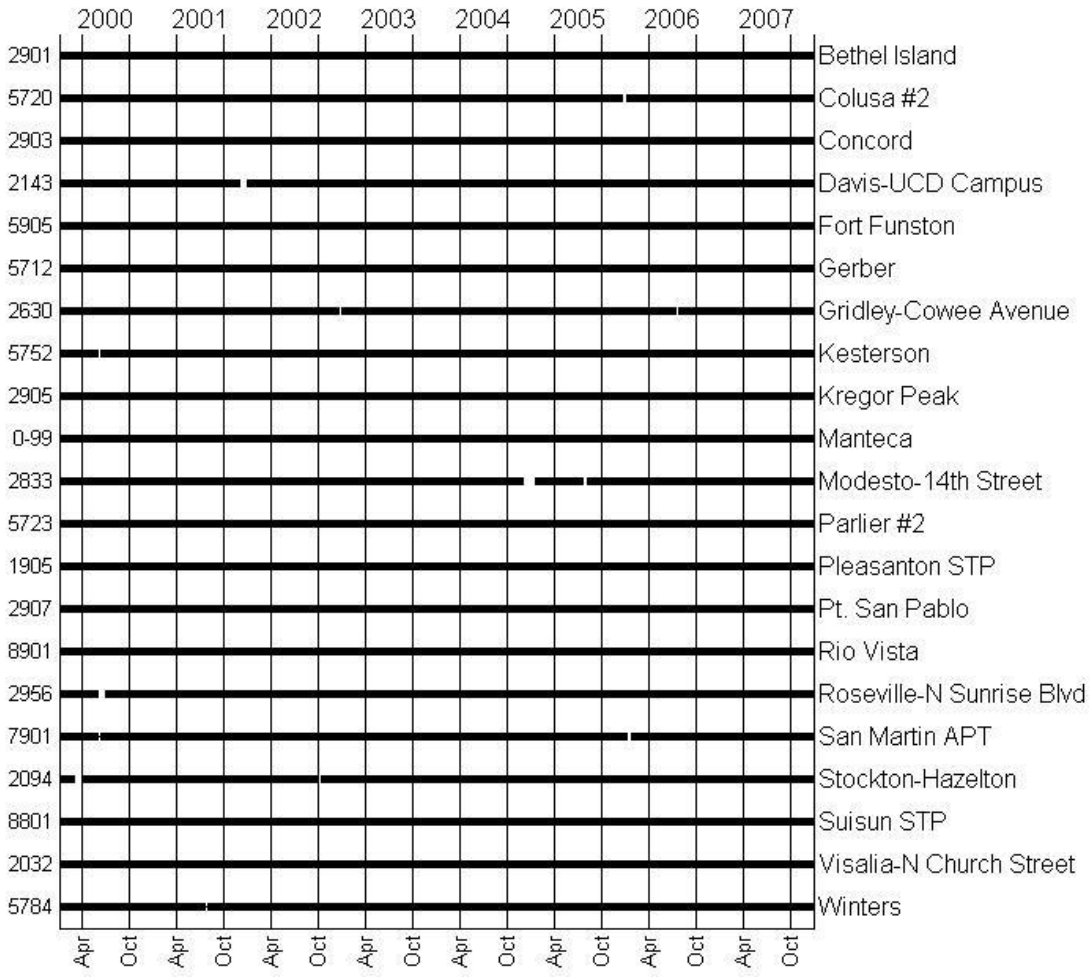

Figure 3. Availability of wind data from weather stations used in the summer transport clustering. Solid horizontal lines indicate periods for which wind data are available for a given station. Vertical lines appear at 1 April and 1 October. Years centered over summer months along top.

Table 4. Names, CARB site codes, and positions for 31 ozone monitors.

Site Name	Site ID	Latitude	Longitude
Redding-Health Dept Roof	2829	40.551	-122.381
Chico-Manzanita Avenue	2115	39.757	-121.842
Willows-E Laurel Street	3137	39.517	-122.190
Colusa-Sunrise Blvd	2744	39.189	-121.998
Yuba City-Almond Street	2958	39.139	-121.619
Roseville-N Sunrise Blvd	2956	38.746	-121.265
Folsom-Natoma Street	3187	38.683	-121.164
Woodland-West Main Street	2490	38.673	-121.788
Woodland-Gibson Road	3249	38.661	-121.731
Sacramento-Del Paso Manor	2731	38.614	-121.368
Davis-UCD Campus	2143	38.535	-121.774
Sloughhouse	3209	38.495	-121.211
Santa Rosa-5th Street	2105	38.444	-122.710
Elk Grove-Bruceville Road	2977	38.303	-121.421
Vallejo-304 Tuolumne Street	2410	38.103	-122.238
Pittsburg-10th Street	2102	38.029	-121.897
Sonora-Barretta Street	2968	37.982	-120.379
San Rafael	2622	37.972	-122.518
Stockton-Hazelton Street	2094	37.952	-121.269
Concord-2975 Treat Blvd	2831	37.939	-122.025
San Francisco-Arkansas Street	2373	37.766	-122.399
Tracy-24081 Patterson Pass Road	3134	37.740	-121.532
Livermore-793 Rincon Avenue	3490	37.688	-121.784
Modesto-14th Street	2833	37.642	-120.994
Turlock-S Minaret Street	2996	37.488	-120.836
Redwood City	2125	37.483	-122.204
San Jose-4th Street	2413	37.340	-121.888
Merced-S Coffee Avenue	3022	37.282	-120.434
Gilroy-9th Street	2320	37.000	-121.575
Clovis-N Villa Avenue	3026	36.819	-119.716
Fresno-1st Street	3009	36.782	-119.773
Parlier	2114	36.597	-119.504
Visalia-N Church Street	2032	36.333	-119.291

4. Results for winter PM

4.1 Winter weather patterns

4.1.1 Clustering results and nomenclature

Clustering was performed for 1001 winter (November-March) days with available measurements from the 9-year study period (1999-2007). Six weather patterns (clusters) were identified having distinct surface air flows, aloft conditions, $PM_{2.5}$ spatial distributions, and particle compositions. Figure 4 shows the assignment of each day of the study period among the six clusters. The clusters usually persisted for 3-5 days when they occurred. This persistence time scale implied significant influences of synoptic (large-scale) circulation patterns to drive the Central California weather. Regional surface conditions usually evolved gradually over the course of several days in response to day-to-day changes in the large-scale aloft conditions.

Composite weather maps of cluster-averaged 500-hPa pressure level geopotential height (Figure 5) indicated the aloft conditions associated with each cluster. The aloft patterns were used to name the clusters: I-R1, I-R2, I-R3, I-R4, I-V, and I-Z. The leading "I-" in each cluster name refers to the "inter-regional" nature of the surface flow patterns and distinguishes the results of this study with those obtained in a previous PM clustering study by Palazoglu, 2009B. The six winter weather patterns depicted three basic aloft large-scale features that could be present on a given day.

- "R" represented an anticyclonic "ridge" of high pressure present at various locations. I-R1, I-R2, I-R3, and I-R4 had ridges located progressively eastward.
- "V" represented a cyclonic trough of low pressure usually over the coastline of California.
- "Z" represented a strongly cyclonic system usually associated with a migrating low pressure cell (storm) at variable position. The low pressure system is generally deeper for Z than V. This feature's name was derived from the mean "zonal" (westerly) aloft flow. The cluster composite for Z (Figure 5) was, however, a mathematical artifact. It resulted from averaging pressure fields across days which exhibited low pressure centers at different locations.

The synoptic features, and numbers and percentages of SFBA 24-hr $PM_{2.5}$ exceedances accounted for by each weather pattern are listed in Table 5. Anticyclonic weather patterns (the four ridging patterns) exhibited decreased dispersion and increased conduciveness for $PM_{2.5}$ buildup.[1] They had relatively little marine intrusion, mostly

[1] Anticyclonic systems are generally associated with sinking (subsiding) and stable air masses. Subsidence generally increases with increased height of aloft pressure levels, and atmospheric stability generally increases with increased aloft (850-hPa level) temperature. They are also likely to exhibit capping thermal inversions at low altitudes. These characteristics inhibit vertical dispersion, trapping pollutants near the ground level. Anticyclonic systems are also generally associated with weak horizontal large-scale pressure

clear-sky conditions (except sometimes for I-R4), winds arriving into the SFBA from the east, and moderate to high Central California $PM_{2.5}$ levels. I-R2 and I-R4 accounted for around 60% and 20% of the SFBA 24-hr $PM_{2.5}$ exceedances (35 $\mu g/m^3$ for 24-hr $PM_{2.5}$ level), respectively.

Typical episodes started with I-R1 conditions, a ridge located offshore and moving toward eastward producing high northerly winds especially in the upper Sacramento valley. I-R1 had moderate $PM_{2.5}$ levels. The ridge was positioned directly over Central California for I-R2 and I-R3 conditions. These conditions are associated with weak large-scale pressure gradients, light and shallow terrain-induced air flows developed locally. I-R3 had a weaker ridge compared to I-R2; therefore, exhibited moderate SFBA $PM_{2.5}$ levels. I-R4 had high winds driven by the large-scale pressure gradient. Limited vertical dispersion under this anticyclonic condition produced elevated $PM_{2.5}$ levels despite the high winds. I-R4 had moderate to high $PM_{2.5}$ levels, depending on location. It often occurred leading out of episodic conditions. The ridge responsible for the episodic conditions (often I-R2) had been displaced inland by a storm approaching California from over the Pacific. The offshore counterclockwise cyclonic motions pushed strong, southerly winds through the Central California terrain.

Strongly cyclonic weather patterns exhibited increased dispersion and decreased conduciveness for $PM_{2.5}$ buildup. I-Z and I-V were purely cyclonic and generally allowed for relatively clean SFBA conditions. Strong, deep, turbulent marine flows were driven through the SFBA by the large-scale pressure gradient. I-Z was often associated with precipitation, whereas I-V was dry.

Figure 6 shows the seasonal distribution of the weather patterns. I-R2, the more frequent episodic pattern, occurred from late November through early February. The seasonality of this weather pattern alone largely accounted for the SFBA "$PM_{2.5}$ season." The less frequent episodic pattern, I-R4, occurred from early November through early March. This pattern accounted for a significant proportion of exceedances outside of the core $PM_{2.5}$ season. I-R3 was strongly anticyclonic; however, it mostly occurred outside of the core $PM_{2.5}$ season. Its seasonality mostly explained its low SFBA exceedance potential. I-R3 may, however, have accounted for the longer $PM_{2.5}$ season in the sheltered Central Valley compared to the coastal SFBA. Conditions were less stable in general than during the coldest winter months due to increased surface heating. I-Z and I-V both occurred frequently throughout the study period. I-V occurred more frequently outside of the core PM season, especially during March. I-Z occurred more frequently from December through February. It largely accounted for the Central California rainy season.

---

gradients. Shallow, terrain-induced low-level air flows associated with aloft anticyclonic conditions have low wind speeds and little turbulence, inhibiting dispersion by mechanical mixing processes.

4.1.2 Surface characteristics

Composite weather maps of cluster-averaged 1000-hPa pressure level geopotential height are shown in Figure 7 and their associated low-level winds at 0500 PST and 1300 PST in Figures 8 and 9, respectively. I-R1, I-R2, I-R3, and I-R4 exhibited a cell of high surface pressure centered northeast of the SFBA (the Great Basin High). This surface high was much stronger for I-R2 than for the other patterns. Each also exhibited a cell of high surface pressure centered west and/or south of the SFBA (the North Pacific High). Orientations of the surface pressure gradients over Central California were largely determined by the relative positions and strengths of the Great Basin and North Pacific Highs. Pressure gradients decreased from north to south for I-R1, from northeast to southwest for I-R2, and from south to north for I-R4. Relative to the other ridging patterns, the North Pacific High was displaced southeast for I-R4 because surface low pressure was expanding southeast from the Gulf of Alaska. I-R4 was a transient cluster that usually represented a storm of arctic origin approaching Central California. For I-R3, the Great Basin and North Pacific Highs had comparable, relatively low pressures. The large-scale pressure gradient over Central California was very weak.

The inland Great Basin High tended to block low-level westerly marine winds from passing through Carquinez Strait. All ridging patterns exhibited easterly winds in the SFBA for at least some hours of the day. I-R1 had northerly flows produced by a large-scale pressure gradient associated with an approaching offshore ridge. Strong winds entered the SV from the north and flowed along its major axis. Flow split at the Delta to enter the SFBA and the SJV. I-R2 and I-R3 had weak large-scale pressure gradients. They exhibited locally generated, terrain-induced flows around the SFBA. Strong nocturnal drainage (downslope) flows over the Central Valley rims converged toward the Central Valley floor, increasing the pressure within the Valley. Air then emptied from the Central Valley to the Pacific Ocean through Carquinez Strait, the only major gap in its surrounding rims. I-R2 had both drainage flows and winds entering the SFBA from the east throughout the day. Light northerly downvalley winds in the SV emptied into the SFBA through Carquinez Strait and pushed further southward into the Santa Clara Valley. SJV conditions were near stagnant. For I-R3, the easterly SFBA flows often reversed to westerly during the afternoon. Central Valley conditions were near stagnant and largely decoupled from the SFBA. I-R4 had southerly flows produced by a large-scale pressure gradient associated with an approaching offshore storm. Winds exited the SJV from the north, entered the SFBA through both Carquinez Strait and Altamont Pass, and pushed further northward into the North Bay valleys. Some of the I-R4 flow split into the SV at the Delta.

Cyclonic patterns I-V and I-Z were dominated by maritime influences and had weak, if any, Great Basin Highs. I-V was most strongly influenced by the North Pacific High. The pressure gradient decreased from west to east. I-Z was most strongly influenced by a cell of arctic low pressure expanded from the Gulf of Alaska over northwestern North America. This dominant arctic influence reflected the stormy nature of I-Z. The pressure gradient decreased from south to north.

I-V exhibited strong, deep, ventilating marine flows entering the SFBA from the west. Wind speeds usually increased during the daylight hours. Flow splitting into the SV and the SJV occurred in the Delta. Much of the strong, turbulent flow passed over the Sierra Range. I-Z exhibited the highest wind speeds and the most unstable, turbulent flows of any pattern. Strong marine winds entering the SFBA from the west converged at the Delta with moderate southerly flows in the SJV. The converged flow entered the SV from the south. The SV winds were also strong. I-Z was a transient pattern. This weather system moved much faster than the other patterns representing Rossby waves associated with the meandering of the jet stream.

Surface temperature patterns (Figure 10) further characterized the low-level air flow patterns. I-R1 had perhaps the most variable temperatures at a given site and sampling hour. I-R1 usually reflected a transition from clean into polluted conditions, and thus experienced a larger range of conditions than the other patterns. I-R2 had the lowest overnight inland temperatures. It also had the sharpest overnight temperature gradient, decreasing from the coast to inland. These observations supported inland nocturnal radiative cooling as the mechanism by which the I-R2 flow pattern developed. I-R3 exhibited considerably higher inland daytime temperatures than the other patterns. Daytime temperatures increased sharply from the coast to inland. The daytime reversal of the I-R3 flows may have resulted from sea breeze development driven by intensified inland surface heating. I-R4 exhibited far less variability in surface temperatures than the other ridging patterns. Both land-sea temperature gradients and day-night temperature changes were relatively small. This pre-storm pattern was windy and often cloudy. High winds helped eliminate temperature spatial gradients, though coastal locations remained slightly warmer than inland overnight. Radiative insulation from the cloud cover reduced the diurnal temperature changes. For the same reasons, stormy pattern I-Z exhibited even less sea-land and day-night temperature differences than I-R4. I-V was cyclonic but not stormy. It exhibited more spatial and diurnal temperature variability than I-Z.

Precipitation patterns (Figure 11) confirmed the stormy nature of I-Z, which accounted for the bulk of the rainy days. It also had the highest levels of precipitation. I-R4 had significant amounts of precipitation, but far less than for I-Z. This pattern usually occurred as a storm approached, but did not yet fully impact, Central California.

4.1.3 Vertical dispersion characteristics

Vertical dispersion characteristics were inferred using 0400 PST Oakland sounding measurements from the 850- and 925-hPa pressure levels (Figure 12) in combination with the above findings.

I-R1 usually represented a transition from cyclonic into episodic conditions. When this cluster occurred over several consecutive days, subsidence and stability increased while mixed layer depth and wind speeds decreased. Though horizontal and vertical dispersion were decreasing, the boundary layer was still significantly deep for dilution of

$PM_{2.5}$ and its precursors to moderate levels. Also, multi-day occurrences of I-R1 usually followed clean conditions. The duration of I-R1 was typically insufficient for adequate pollutant accumulation (carry over) and air mass aging to allow SFBA $PM_{2.5}$ levels to build from near-background levels to the exceedance level. Episodes instead usually occurred immediately after I-R1 transitioned into a fully episodic weather pattern.

I-R2 had the highest 850-hPa geopotential heights (pressures), suggesting a strongly subsiding air mass. They were on average around 25 m higher than for I-R1 and I-R3, which had moderate degrees of subsidence. I-R4 and I-V had somewhat lower heights and likely lacked significant subsidence. The very low pressures for I-Z suggested a lifting, turbulent air mass.

I-R1 had relatively cool surface temperatures, a slightly increasing vertical temperature gradient, and a resulting stable air mass. I-R2 and I-R3 had elevated temperatures at the 925-hPa level that were considerably warmer than nearby surface locations during the overnight hours (see Figure 10). Both clusters exhibited strongly stable boundary layers. They also likely had capping thermal inversions at very low levels. I-R3 aloft temperatures were on average 1-2 degree C warmer than I-R2, but its surface temperatures were at least several degrees warmer. I-R2, with sharply increasing vertical temperature gradient, had the most strongly stable boundary layer. I-R4, I-V, and I-Z had relatively warm surface temperatures, decreasing vertical temperature gradients, and lacked strong stability. I-Z had the warmest overnight surface temperatures and the lowest aloft temperatures. Conditions were unstable and turbulent.

I-R1 exhibited strong aloft airflows. Aloft *u* (westerly) and *v* (southerly) wind components confirmed the localized nature of the I-R2 and I-R3 surface winds. Their aloft winds were very weak. The possibly polluted surface layer was decoupled from the upper levels. The shallow flows, possibly associated with low-level thermal inversions, trapped pollutants near the surface. Strong aloft flows for I-R4, I-V, and I-Z were from the south, west, and southwest, respectively. These patterns had aloft winds with similar directions and higher speeds compared to their respective bulk surface flows through the complex Central California terrain. The surface was coupled with the aloft levels and air flows were deep. The deep mixed layers allowed the potential for pollutant dispersion away from the surface; however, surface ventilation required a sufficient rate and duration for the vertical dispersion to operate.

I-R4 usually represented a rapid transition from episodic into stormy conditions. When this cluster occurred, subsidence and stability decreased dramatically while mixed layer depth and wind speeds increased sharply. Pollutants that were accumulated under episodic conditions prior to the occurrence of I-R4, however, typically remained near the ground level during the brief occurrences of I-R4. The mixed layer was likely sufficiently deep to disperse the pollutants; however, the rate of vertical dispersion was too slow to achieve a well-mixed boundary layer during the transient I-R4 occurrences.

The strong horizontal winds for I-R4 transported the previously accumulated pollutants in the SJV considerable distances before a transition into fully cyclonic, adequately ventilated conditions occurred.

Vertical profiles in the boundary layer were quite different for I-Z compared to the other clusters. A large-scale wake resulted over Central California as the fast-moving, unstable I-Z air mass impinged on the Coast Range and then the Sierra Range. The generated turbulence provided coupling between the clean, aloft air mass and the polluted air mass within the sheltered valleys of the complex Central California terrain. $PM_{2.5}$ and precursors were rapidly scoured from the surface before appreciable low-level advection could occur.

4.2 Inter-regional air quality patterns

4.2.1 $PM_{2.5}$ spatial patterns

Total 24-hr $PM_{2.5}$ levels are shown for five SFBA sites and seven Central Valley sites in Figure 13. Approximately 60% of the San Jose $PM_{2.5}$ measurements from I-R2 days exceeded the 24-hr $PM_{2.5}$ standard (35 $\mu g/m^3$). Thus, I-R2 was associated with an at least 60% probability of triggering a SFBA exceedance when it occurred. This is a lower bound because measurements were not available for all I-R2 days. At least 25% of the I-R4 days resulted in exceedances in the east SFBA. The other patterns were not very likely to produce 24-hr $PM_{2.5}$ exceedances in the SFBA. I-R1 and I-R3 had moderate SFBA $PM_{2.5}$ levels. I-V and I-Z had low SFBA $PM_{2.5}$ levels that were typically below the annual $PM_{2.5}$ standard (15 $\mu g/m^3$).

I-R2 exhibited the highest $PM_{2.5}$ levels throughout Central California. SFBA I-R2 levels peaked at San Jose. I-R4 generally had the next-highest $PM_{2.5}$ levels. SFBA $PM_{2.5}$ levels were highest in the East Bay and relatively low at the other sites. SJV $PM_{2.5}$ levels were relatively high. For I-R3, the Central Valley $PM_{2.5}$ levels were generally comparable with I-R4. The SFBA was largely decoupled from the Central Valley, and SFBA $PM_{2.5}$ levels were moderate. SFBA I-R3 $PM_{2.5}$ levels were higher than for I-R4 except in the East Bay. I-R1 had moderate $PM_{2.5}$ levels in the SFBA and SV and high $PM_{2.5}$ levels in the SJV. $PM_{2.5}$ levels for I-V were low to moderate in northern SJV and low elsewhere. I-Z $PM_{2.5}$ levels were low for all locations.

4.2.2 $PM_{2.5}$ composition

The dominant $PM_{2.5}$ components (Figure 14) at all sites were carbonaceous material (OC plus EC) and ammonium nitrate (measured as nitrate plus most of the ammonium). Sulfate levels were generally quite low; however, 1-3 $\mu g/m^3$ sulfate were present in the SFBA and the SJV during I-R2 and in the SJV only for I-R4.

The SJV exhibited the highest ammonium nitrate levels. They were on average around twice as high as in the SFBA or around Sacramento. SJV ammonium nitrate levels were highest for I-R2, followed by I-R3, then I-R4. The SJV $PM_{2.5}$ may have been most strongly

impacted by emissions of NO_x and ammonia. The SJV conditions for I-R2 and I-R3 were highly conducive to the transformation of NO_x into nitric acid. Winds were diurnally calm, the days were clear and sunny, and the nights were cool, humid, and often foggy. The SJV also had intense ammonia emissions, much from dairies. The ammonia rapidly consumed the available nitric acid to form ammonium nitrate particulate. The cooler temperatures of I-R2 compared to I-R3 favored more accumulation of the locally formed ammonium nitrate.

I-R4 usually represented a transition from polluted into stormy conditions. The strong southerly winds advected the carried over ammonium nitrate out of the SJV and through the SFBA and SV. Ammonium nitrate levels were still high in the SJV, but the conditions were not very conducive to additional formation. Some days exhibited higher Modesto ammonium nitrate levels for I-R4 than I-R3. This was because ammonium nitrate that had accumulated to high levels deeper into the SJV was transported past Modesto, in the northern SJV, by the southerly air flow. A similar argument was likely for the relatively high Modesto sulfate levels for I-R4.

OC levels in the SJV were highest for I-R2, the pattern with the least vertical dispersion. The other ridging patterns had similar OC levels that were generally well below the I-R2 levels. This pattern probably mostly reflected locally emitted OC, whose levels varied with degree of vertical dispersion. Occasionally, I-R1 and I-V had spuriously high OC levels in the SJV. This pattern may have reflected transported OC from the Sacramento area. EC data were not available for the northern SJV.

The Sacramento area exhibited the highest carbonaceous $PM_{2.5}$ levels. OC levels were especially higher than for the other areas. The Sacramento area $PM_{2.5}$ may have been most strongly impacted by wood burning, cooking, fossil fuels combustion, and biogenic emissions. Sacramento area carbonaceous $PM_{2.5}$ levels were high for I-R2 and moderate for the other ridging patterns. For I-R2, accumulation of locally emitted and advection of carbonaceous material from the upper Sacramento valley (mostly from wood burning) contributed to high levels of PM around Sacramento. I-R2 also had moderate ammonium nitrate levels there. This ammonium nitrate could have been locally formed and/or regionally accumulated under the relatively calm Central Valley conditions. The I-R2 flow pattern transported these accumulated pollutants in the Sacramento area to the SFBA. Ammonium nitrate was unlikely to have been transported from the SJV into the SV except for under I-R4. This pattern occasionally had high ammonium nitrate levels around Sacramento. The transported ammonium nitrate was then rapidly ventilated during the onset of the storm following I-R4.

The SFBA $PM_{2.5}$ composition varied with the conditions. I-R2 and I-R3 had relatively high and moderate levels, respectively, for both carbonaceous material and ammonium nitrate. The high levels for I-R2 resulted from a combination of local emissions and transport from the Sacramento area. I-R3 usually did not exhibit significant transport. This was evidenced by the disparity between the high Central Valley and low SFBA total

$PM_{2.5}$ levels for I-R3 (see Figure 13). The diurnally reversing I-R3 winds likely circulated accumulated $PM_{2.5}$ around the SFBA. The afternoon marine flows were insufficient to completely ventilate the region. The I-R3 $PM_{2.5}$ was a combination of local pollutants and also $PM_{2.5}$ that was transported and carried over from previous days (e.g. under I-R2).

Occasionally, I-R3 exhibited spuriously high SFBA ammonium nitrate levels without carbonaceous $PM_{2.5}$ levels spiking. Likely for these days, the I-R3 SFBA easterly flows extended into areas of the Delta nearest the SFBA. Regionally accumulated ammonium nitrate from the Delta may have been transported into the SFBA. The I-R3 flow pattern did not extend as far as the Sacramento, Stockton, or Modesto source areas. Therefore, an insignificant amount of primary $PM_{2.5}$ was likely transported into the SFBA by I-R3.

I-R1 also exhibited occasionally spuriously high SFBA ammonium nitrate and carbonaceous $PM_{2.5}$ levels. These events may have represented anomalous transport from the Sacramento area. Likely, these events occurred as the mixed layer and vertical dispersion had decreased near a transition into a fully episodic pattern.

Ammonium nitrate levels measured at San Jose were low for I-R4; however, high levels of ammonium nitrate and possibly other pollutants were transported into the East Bay during I-R4 occurrences. Likely, East Bay ammonium nitrate levels under I-R4 were comparable with those from Modesto in the SJV, from where the transported ammonium nitrate originated.

Levels for trace $PM_{2.5}$ components are shown in Figure 15. They helped confirm the proposed source-receptor relationships for the weather patterns. Geological dust (silicone) levels in the SFBA were elevated for I-R1, I-R2, and I-R3. These patterns had winds arriving into the SFBA from upwind inland locations. Marine aerosol (suspended sodium and chlorine) levels were highest for I-V and I-Z, the patterns with strong marine flows. Soluble sodium levels in the Central Valley were well below those observed in the SFBA. $PM_{2.5}$ was indeed transported into the Central Valley from the SFBA under cyclonic conditions; however, the pollutants were mostly vertically dispersed to low levels by the turbulent flows of the possibly unstable air masses. The transport impacts of I-V and I-Z were likely usually small or negligible. I-R4 had the lowest levels of marine aerosol and geological dust. These naturally occurring $PM_{2.5}$ trace components may have had larger particle diameters than for the ammonium nitrate or carbonaceous material. Thus, significant deposition of the trace components may have occurred under I-R4 during their near-surface transport over large distances.

4.3 Evolution of $PM_{2.5}$ episodes

Figure 16 depicts three pathways describing idealized evolutions of weather patterns associated with SFBA $PM_{2.5}$ episodes. The diagram indicates all transitions that were favored at moderate to high levels of confidence.

Most $PM_{2.5}$ episodes developed as an offshore ridge approached Central California (i.e. pattern I-R1). The clockwise motion under the leading (eastern) edge of the ridge produced strong, deep northerly winds that entered the SV from the north and mostly exited the Central Valley through the SFBA. Transport into the SFBA under I-R1 was not very significant because of the strong, deep flow pattern. I-R1 was more likely to have transported pollutants from the Sacramento area into the SJV where conditions were stagnating. The I-R1 pattern was often preceded by clean I-V conditions.

When I-R1 occurred, it almost always transitioned into I-R2 as the ridge advanced eastward over Central California. Easterly winds continued to enter the SFBA under I-R2, and the flow became much more shallow and light than for I-R1. Pollutants were accumulated near the surface and transported from the Sacramento area through the central SFBA and into the Santa Clara Valley. Transport from the Sacramento area was likely to exhibit a large fraction of locally emitted carbonaceous material, in addition to regionally accumulated ammonium nitrate. Transport into the SJV under I-R2 was unlikely; however, the SJV air mass was calm and aged rapidly to form and accumulate ammonium nitrate.

I-R2 was a relatively persistent pattern. Episodes would generally persist until a transition into a cyclonic pattern occurred, perhaps involving a transient, intermediate occurrence of I-R4. Different transitions out of I-R2 defined three types of episodes, as shown in Figure 16 and discussed in the subsections below. I-R3 does not appear in Figure 16 and is not discussed in this section because it mostly occurred outside the SFBA $PM_{2.5}$ season. It was not representative of SFBA episodes.

4.3.1 Gradually terminating episodes

The upper pathway in Figure 16 (involving I-R2→I-V) indicated a gradual evolution from strongly anticyclonic, usually episodic conditions, into cyclonic conditions. Significant transport of $PM_{2.5}$ from the Sacramento area usually occurred under I-R2. This type of episode terminated as an offshore trough gradually pushed eastward to displace the ridge over Central California. The cumulative transport impacts for this type of episode were often high. This was because I-R2 could persist for potentially long periods until a sufficiently deep trough advanced from over the Pacific Ocean to near the California coastline. Anticyclonic blocking associated with I-R2 served to retard troughs from approaching the coastline. The I-R2 episodic conditions were self-sustaining, and episodes of long durations were common.

The onset of I-V was marked by marine air intrusion through the SFBA and into the Central Valley. SFBA $PM_{2.5}$ levels often remained elevated for up to several days before clean conditions were achieved. During this initial period of decreasing $PM_{2.5}$ levels, transport from the SFBA into the Central Valley was possible. Usually, this transport may have been minimal or negligible because the Central Valley was mostly ventilated of accumulated $PM_{2.5}$ by the strong, turbulent winds.

4.3.2 Rapidly terminating episodes

The middle pathway in Figure 16 (involving I-R2→I-Z) indicated a rapid evolution from strongly anticyclonic, usually episodic conditions into intensely cyclonic conditions. Significant transport of $PM_{2.5}$ from the Sacramento area into the central SFBA usually occurred under I-R2. This type of episode terminated as the front of a migrating offshore storm rapidly approached and possibly blew over Central California. The fast-moving I-Z system was able to displace even the most intensely anticyclonic ridges from over Central California. As such, strongly episodic ridges (I-R2) that may have persisted in the absence of a storm were displaced eastward or otherwise dissipated. Storms diminished the persistence of I-R2, reducing the cumulative transport impact from the Sacramento Area into the SFBA.

The onset of I-Z was marked by rapid marine intrusion and increased vertical dispersion. SFBA $PM_{2.5}$ levels decrease rapidly, often achieving clean conditions over 1-2 days. Central Valley likewise experienced a rapid ventilation of accumulated $PM_{2.5}$ by the strong, turbulent air flows and unstable conditions. Inter-regional transport under I-Z was unlikely because of the strong vertical dispersion.

4.3.3 Episodes with transport from the SJV

The bottom pathway in Figure 16 (involving I-R2→I-R4→I-Z) was similar to the middle pathway discussed in section 4.3.2. The difference is that I-R4 occurred intermediate of the persisting I-R2 episode and the stormy conditions. While I-R2 persisted, the SJV conditions were calm and conducive to ammonium nitrate buildup to high levels. I-R4 occurred as a storm approached the coastline. It produced southerly aloft flows over Central California and low surface pressure in the SV. Strong southerly surface winds in the SJV transported the accumulated pollutants northward into the SFBA and the SV. The East Bay and North Bay were affected by transported regionally accumulated $PM_{2.5}$ that was mostly ammonium nitrate. The occurrences of I-R4 were often brief; however, overwhelming levels of transport from the SJV into the SFBA sometimes occurred. In most cases, the transport impacts on the SFBA were at least significant.

The I-R4→I-Z transition marked the point at which the storm reached Central California. Much of the accumulated $PM_{2.5}$ throughout Central California had already been advected away by the strong I-R4 surface winds. The unstable and turbulent conditions associated with the onset of I-Z provided sufficient vertical dispersion to quickly ventilate much of the remaining $PM_{2.5}$. Heavy precipitation associated with I-Z may have also provided for significant wet deposition of pollutants. Clean conditions were often achieved immediately after the transition into I-Z.

4.4 Transport potential for $PM_{2.5}$ and precursors

Patterns I-R2 and I-R4 were most likely to exhibit significant transport into the SFBA from the Central Valley. They accounted for around 60% and 20% of SFBA 24-hr $PM_{2.5}$ exceedance days, respectively. Transport impacts typically ranged from significant to

overwhelming during the SFBA exceedances under I-R2 and I-R4. The less frequent transport pattern, I-R4, may have been associated with higher levels of transported $PM_{2.5}$ on the days that it occurred. The more frequent transport pattern, I-R2, may have been associated with greater cumulative transport impacts (totaled over multiple days).

I-R2 had transport mostly from the Sacramento area. This transport occurred primarily through Carquinez Strait. This transported $PM_{2.5}$ likely had a large fraction of locally emitted carbonaceous material, in addition to regionally accumulated ammonium nitrate. The transport appeared to have affected the central SFBA (San Jose monitoring location) most strongly. The East Bay may have also been affected. Transport from the SJV may have also occurred through Altamont Pass during I-R2.

I-R4 had transport mostly from the SJV. This transport occurred through both the Altamont Pass and Carquinez Strait. This transported $PM_{2.5}$ was dominated by ammonium nitrate. The ammonium nitrate usually accumulated in the SJV under other ridging patterns that occurred prior to I-R4, especially I-R2. The transport usually only affected the East Bay, where high $PM_{2.5}$ levels occurred, and also the North Bay. San Jose usually did not appear to be strongly impacted.

There was some evidence for significant transport to infrequently occur into the SFBA for I-R1. These potential transport events were not representative. The Central Valley was upwind of the SFBA for I-R1; however, the flows were too deep and windy for significant transport to have occurred. This pattern likely resulted in significant transport from the Sacramento area into the SJV. The SJV $PM_{2.5}$ resulting from transport may possibly have subsequently been transported into the SFBA.

The SFBA and the Central Valley were largely decoupled for I-R3. Occurrences of I-R3 were, however, associated with significant formation and accumulation of ammonium nitrate in the SJV. I-R3 usually occurred outside of the SFBA $PM_{2.5}$ season. As such, the late-season $PM_{2.5}$ buildup in the SJV was relatively inconsequential to the SFBA 24-hr $PM_{2.5}$ attainment status. This late-season inland $PM_{2.5}$ buildup could become relevant if the 24-hr $PM_{2.5}$ standard is lowered, such that the SFBA $PM_{2.5}$ season is extended into late February or even March.

Pattern I-Z had westerly air flows through the SFBA and into the Central Valley; however, transport potential for this weather pattern was likely very low and inconsequential. The turbulent, unstable conditions produced a very high vertical dispersion rate. Despite the strong surface winds, accumulated pollutants were usually dispersed upward before significant transport could occur. There was no flow splitting at the Delta. Any transport that did occur from the SFBA was likely into the SV.

Transport from the SFBA into the Central Valley was possible; however, such transport occurred less frequently and to a much lower degree than transport into the SFBA. I-V appeared to have the most transport potential from the SFBA. This pattern could have

potentially transported pollutants deep into both the SV and the SJV. It is possible that afternoon marine flows for I-R3 may have transported pollutants from the SFBA into the Delta region.

SFBA NO_x transported into the Central Valley likely impacted Central Valley $PM_{2.5}$ levels more strongly than for other SFBA emissions types. Transported, aged NO_x may have reacted rapidly with locally emitted ammonia in the Central Valley to form ammonium nitrate. It is unclear how much of the Central Valley ammonium nitrate may have resulted from SFBA NO_x emissions. If significant, the Central Valley ammonium nitrate resulting from SFBA NO_x emissions may have been transported back to the SFBA. Ammonia transport from the SFBA was unlikely because sufficient nitric acid was usually present to consume ammonia near its sources. Transport of carbonaceous material from the SFBA into the Central Valley was unlikely to be highly significant. Carbonaceous $PM_{2.5}$ tended to accumulate locally around its sources and was not regionally accumulated in the SFBA.

4.5 Case studies

Three case studies of SFBA $PM_{2.5}$ episodes involving transport from the Central Valley are provided. Each case study depicts one of the idealized evolutions of weather patterns shown in Figure 16.

4.5.1 A gradually terminating episode

Figure 17 shows a gradually terminating episode. It fits the conceptual model described in section 4.3.1 and is depicted by the upper pathway of Figure 16. Time series for the weather patterns and $PM_{2.5}$ levels are shown for 19 December 1999 through 2 January 2000. The episode followed the I-R1→I-R2→I-V sequence of weather patterns.

The episode developed as an offshore ridge of high pressure approached the California coastline. SFBA $PM_{2.5}$ levels slowly built to above 20 $\mu g/m^3$ while I-R1 persisted. Sacramento area $PM_{2.5}$ levels were generally around 40-50 $\mu g/m^3$ while I-R1 persisted. (The spike in Sacramento area $PM_{2.5}$ levels on 20 December was not explained by the conceptual model and may have represented a local emissions event.) Very high $PM_{2.5}$ levels (around 100 $\mu g/m^3$) were achieved in SJV. Transport may have occurred into the SJV from the Sacramento area.

The I-R1→I-R2 transition occurred over 21-23 December, during which $PM_{2.5}$ levels increased dramatically throughout Central California. I-R2 persisted for about a week through 27 December. Initially when I-R2 occurred, SFBA $PM_{2.5}$ levels were 2-3 times lower than in the Central Valley. While I-R2 persisted, the Central Valley $PM_{2.5}$ levels remained approximately constant. SFBA $PM_{2.5}$ levels, however, increased over the next several days due to a combination of transported and locally accumulated $PM_{2.5}$. Transport mostly occurred from the Sacramento area, and SFBA $PM_{2.5}$ levels increased

to similar levels as around Sacramento. SJV $PM_{2.5}$ levels remained higher than for the other regions because of the near calm conditions.

Central California $PM_{2.5}$ levels started to decrease slightly in advance of the I-R2→I-V transition that occurred over 29-30 December. $PM_{2.5}$ levels decreased at about the same rate throughout Central California through 31 December. From this point, I-V persisted while a trough was positioned over the California coastline. SFBA $PM_{2.5}$ levels continued to decrease to low levels in response to the marine ventilation. Central Valley $PM_{2.5}$ levels, on the other hand, stopped decreasing and remained at moderate levels. The lack of further reductions in the Central Valley $PM_{2.5}$ levels may have resulted from insufficient marine air penetration and/or pollutant transport from the SFBA.

4.5.2 A rapidly terminating episode

Figure 18 shows a rapidly terminating episode. It fits the conceptual model described in section 4.3.2 and is depicted by the middle pathway of Figure 16. Time series for the weather patterns and $PM_{2.5}$ levels are shown for 29 November through 10 December 2006. The episode followed the I-R1→I-R2→I-Z sequence of weather patterns.

The development of the episode was similar as for the gradually terminating episode described in section 4.5.1 and shown in Figure 17. I-R1 persisted leading into the episode. $PM_{2.5}$ levels were generally moderate and peaked in the relatively calm SJV. I-R2 then persisted for around a week while exceedances occurred. Sacramento area and SJV $PM_{2.5}$ levels increased sharply around the I-R1→I-R2 transition ending on 1 December. $PM_{2.5}$ levels for these inland regions then held roughly constant while I-R2 persisted. Transport mostly occurred from the Sacramento area, and SFBA $PM_{2.5}$ levels increased to similar levels as around Sacramento after about two days. SJV $PM_{2.5}$ levels remained somewhat higher than for the other regions because of the near calm conditions.

Central California $PM_{2.5}$ levels decreased sharply after the I-R2→I-Z transition ending on 8 December. $PM_{2.5}$ levels decreased at similar rates throughout Central California. The following day, $PM_{2.5}$ had been scoured to low levels throughout Central California. The uniformly and rapidly decreasing $PM_{2.5}$ levels throughout Central California evidenced the ventilating effects of vertical dispersion. The strong horizontal winds were unlikely to have transported a significantly polluted air mass. The inland $PM_{2.5}$ levels responded similarly as for the coastal locations because of the high dispersion rate of I-Z.

4.5.3 An episode with transport from the SJV

Figure 19 shows an episode that terminated with overwhelming transport from the SJV. It fits the conceptual model described in section 4.3.1 and is depicted by the lower pathway of Figure 16. Time series for the weather patterns and $PM_{2.5}$ levels are shown for 25 December 2000 through 12 January 2001. The episode followed the I-R1→I-R2→I-R4→I-Z sequence of weather patterns.

The development of the episode was similar as for the episodes described in sections 4.5.1 and 4.5.2 and shown in Figures 17 and 18, respectively. I-R1 persisted leading into the episode. $PM_{2.5}$ levels were generally moderate and peaked in the relatively calm SJV. An extremely anticyclonic I-R2 weather pattern then persisted for nearly two weeks while exceedances occurred. Transport from the Sacramento area likely contributed significantly to the SFBA $PM_{2.5}$ levels. These extremely conducive conditions produced some of the highest SFBA $PM_{2.5}$ levels observed during the study period. San Jose $PM_{2.5}$ levels were especially elevated relative to the other SFBA locations during much of the I-R2 occurrence. In the SJV, $PM_{2.5}$ accumulated to high levels largely due to ammonium nitrate formation and buildup.

Most locations exhibited a spike in $PM_{2.5}$ levels occurring on 1 January. Likely, this was a result of increased household emissions on the New Year holiday.

The I-R2→I-R4 transition occurred as a storm approached California. The winds shifted to southerly. Pollutants were transported northward, especially from the SJV where regional secondary $PM_{2.5}$ levels were highest. The southerly flow transported the polluted SJV air mass northward through Altamont Pass, Carquinez Strait, and the Delta. Sacramento area and east SFBA locations (Concord and Livermore) were heavily impacted. The central SFBA was outside of the plume extending northward from the SJV. San Jose area pollutants were transported to the north and west to ventilate the central SFBA. Before the transition into I-R4 occurred, south and east SFBA $PM_{2.5}$ levels were roughly uniform at around 70 $\mu g/m^3$. The next day, east SFBA $PM_{2.5}$ levels increased by around 20-30 $\mu g/m^3$ while south SFBA $PM_{2.5}$ levels decreased by around 50 $\mu g/m^3$. The SFBA emissions alone could not possibly have explained this disparity of around 70 $\mu g/m^3$ $PM_{2.5}$ between the South Bay and East Bay. The I-R4 air flow pattern provided an overwhelming degree of transport into the SFBA from upwind locations on 7 January. It is likely that an exceedance would have occurred in the SFBA on this day without any local emissions.

On the following day, 8 January, the storm reached Central California. $PM_{2.5}$ levels were immediately reduced to low to moderate levels throughout Central California. At this point, the $PM_{2.5}$ that accumulated mostly during the episodic I-R2 occurrence had either been advected away from Central California under I-R4 or dispersed vertically by the storm (I-Z). Sustained transport by the strong I-Z surface winds was unlikely. $PM_{2.5}$ levels remained low.

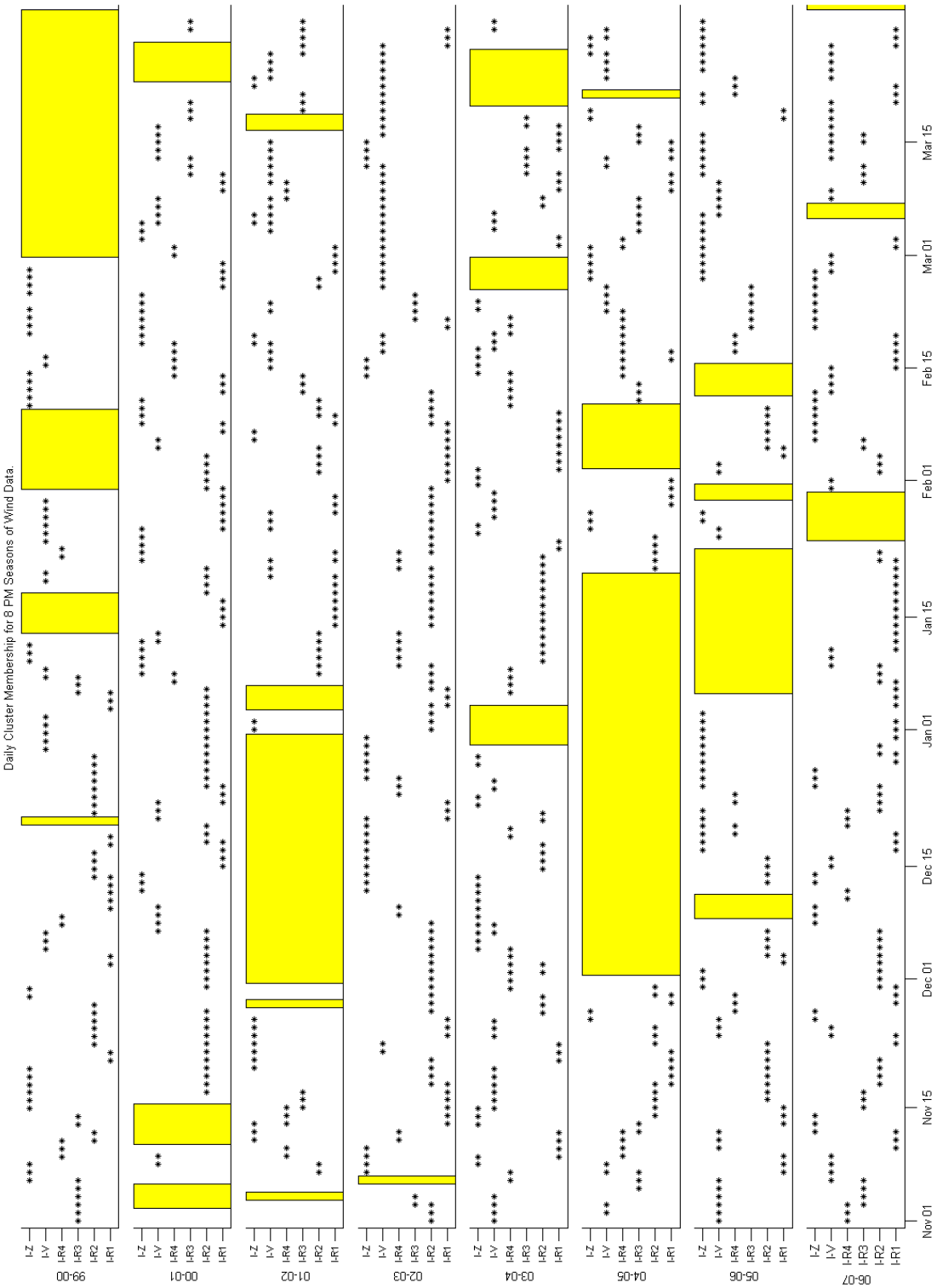

Figure 4. Cluster assignments for 1 November through 31 March of 1999-2007 winter study period. Y-axis position of each marker indicates a cluster assignment for that day. Tick marks (from bottom to top) correspond to clusters I-R1, I-R2, I-R3, I-R4, I-V, and I-Z. Days blocked out in yellow were excluded from the cluster analysis.

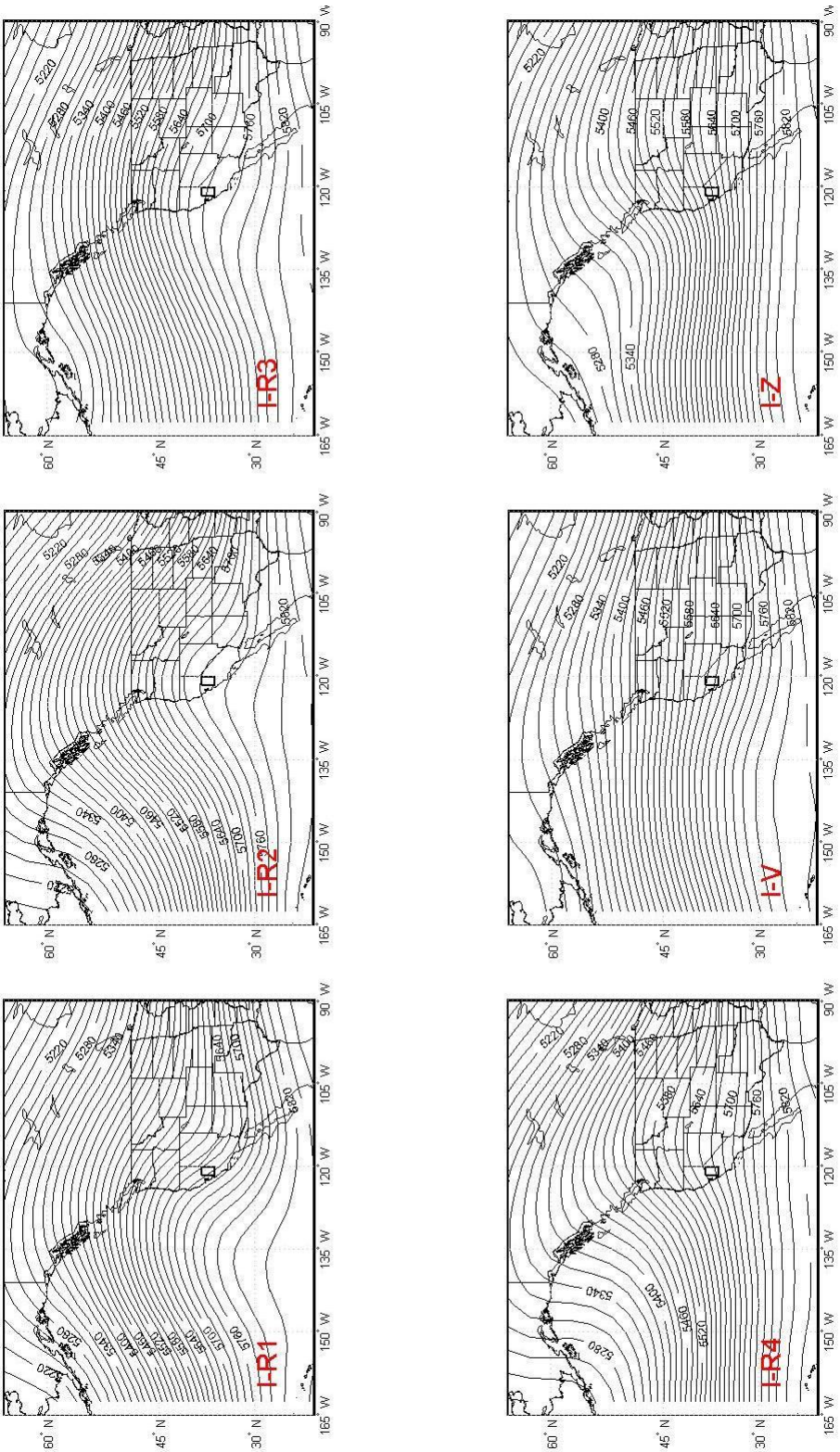

Figure 5. Composite 1800 UTC 500-hPa weather maps for winter clusters, averaged among the days assigned to each cluster. Contours are spaced at 10 m intervals and labeled every 40 m.

Table 5. Names, number of days assigned, number of SFBA 24-hr $PM_{2.5}$ exceedance days, proportion of SFBA 24-hr $PM_{2.5}$ exceedances accounted for (of 136 total during the study period), and synoptic features for 6 winter clusters.

Cluster Label	# of days	Exceedances	% exceedances accounted for	Synoptic feature(s)
I-R1	191	9	6	Offshore ridge
I-R2	220	104	60	Onshore ridge
I-R3	81	3	2	Onshore ridge (weak pressure gradient)
I-R4	97	14	20	Inland ridge
I-V	203	7	5	Coastal trough
I-Z	219	5	4	Migratory storm/cyclone

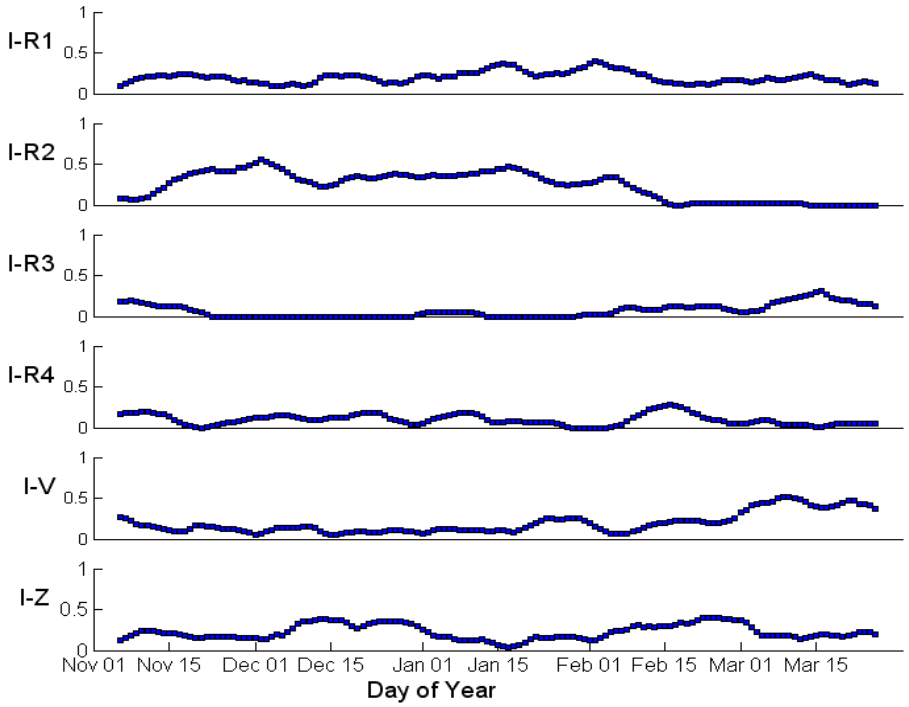

Figure 6. Seasonal distribution for 6 winter clusters. Curves indicate historical frequencies of occurrence for the clusters across the winter season.

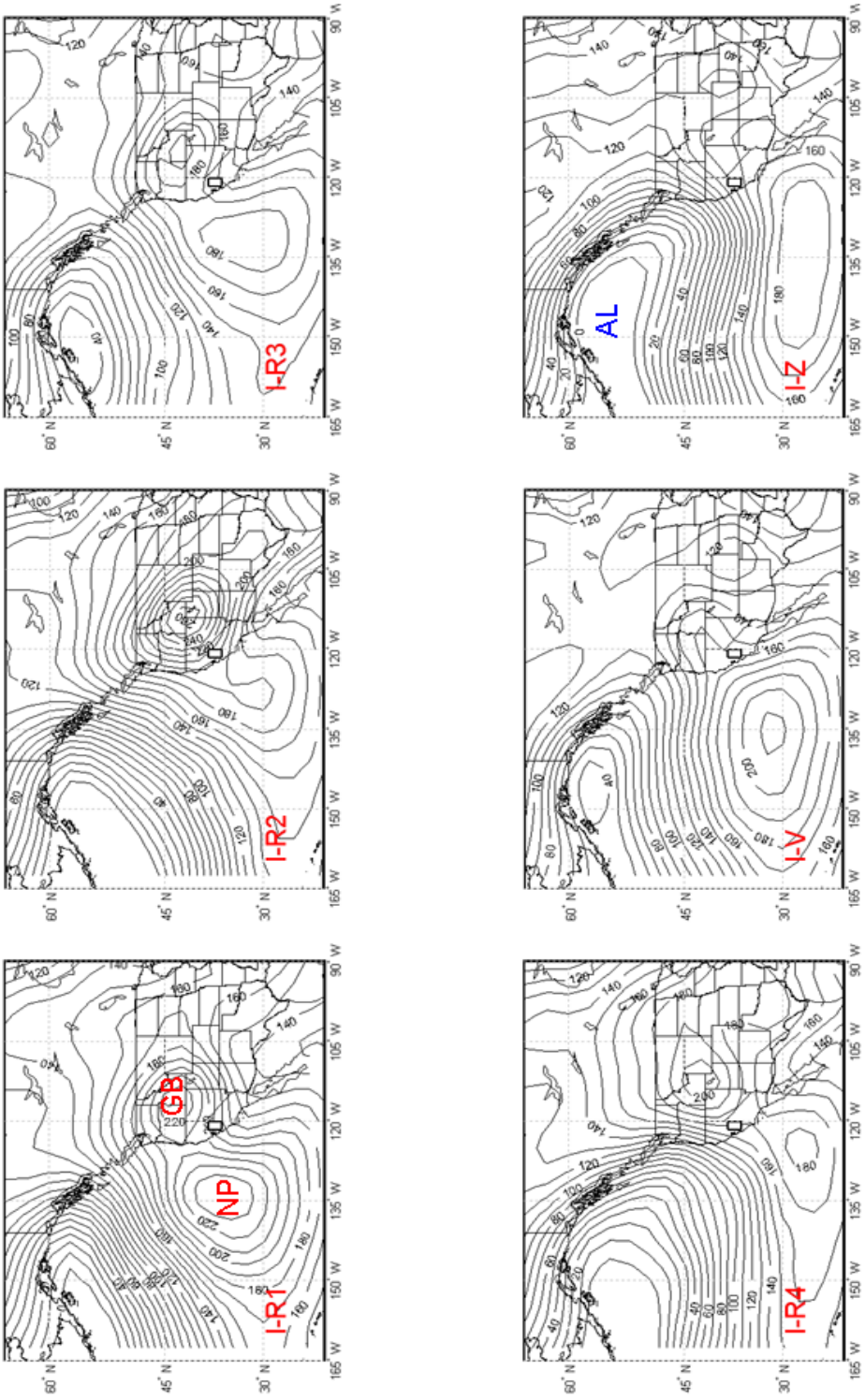

Figure 7. Composite 1800 UTC 1000-hPa weather maps for winter clusters, averaged among the days assigned to each cluster. Contours are spaced at 10 m intervals and labeled every 20 m. “GB”, “NP”, and “AL” indicate positions of the Great Basin High, the North Pacific High, and Aleutian low pressure systems, respectively. Each of these features is shown for only a single cluster for clarity.

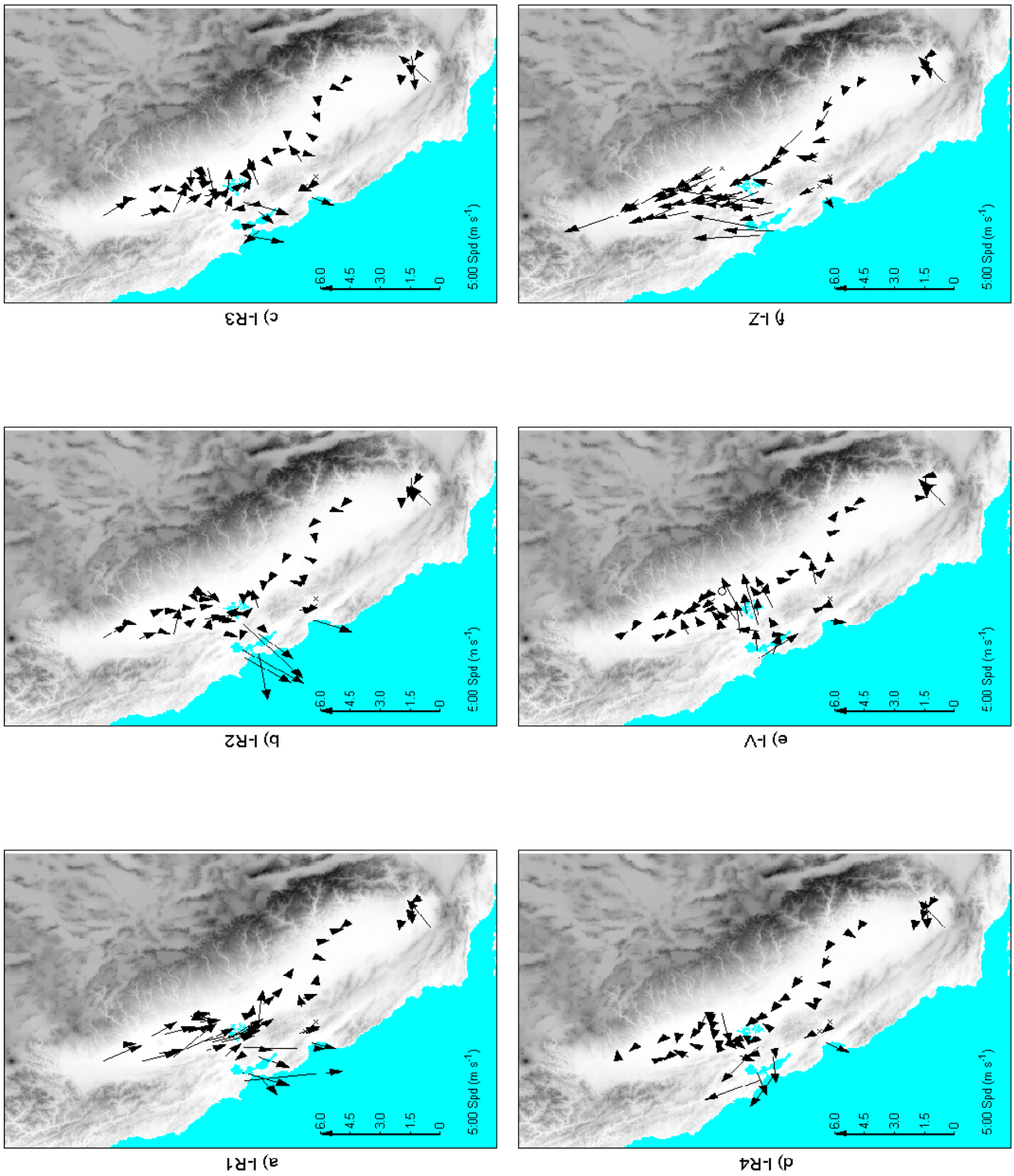

Figure 8. Mean 0500 PST surface wind fields for 6 winter clusters, shown for SFBA and Central Valley monitors. Length of arrow is proportional to mean wind speed, as indicated on scale. Arrows point along wind direction, with tail at weather station position.

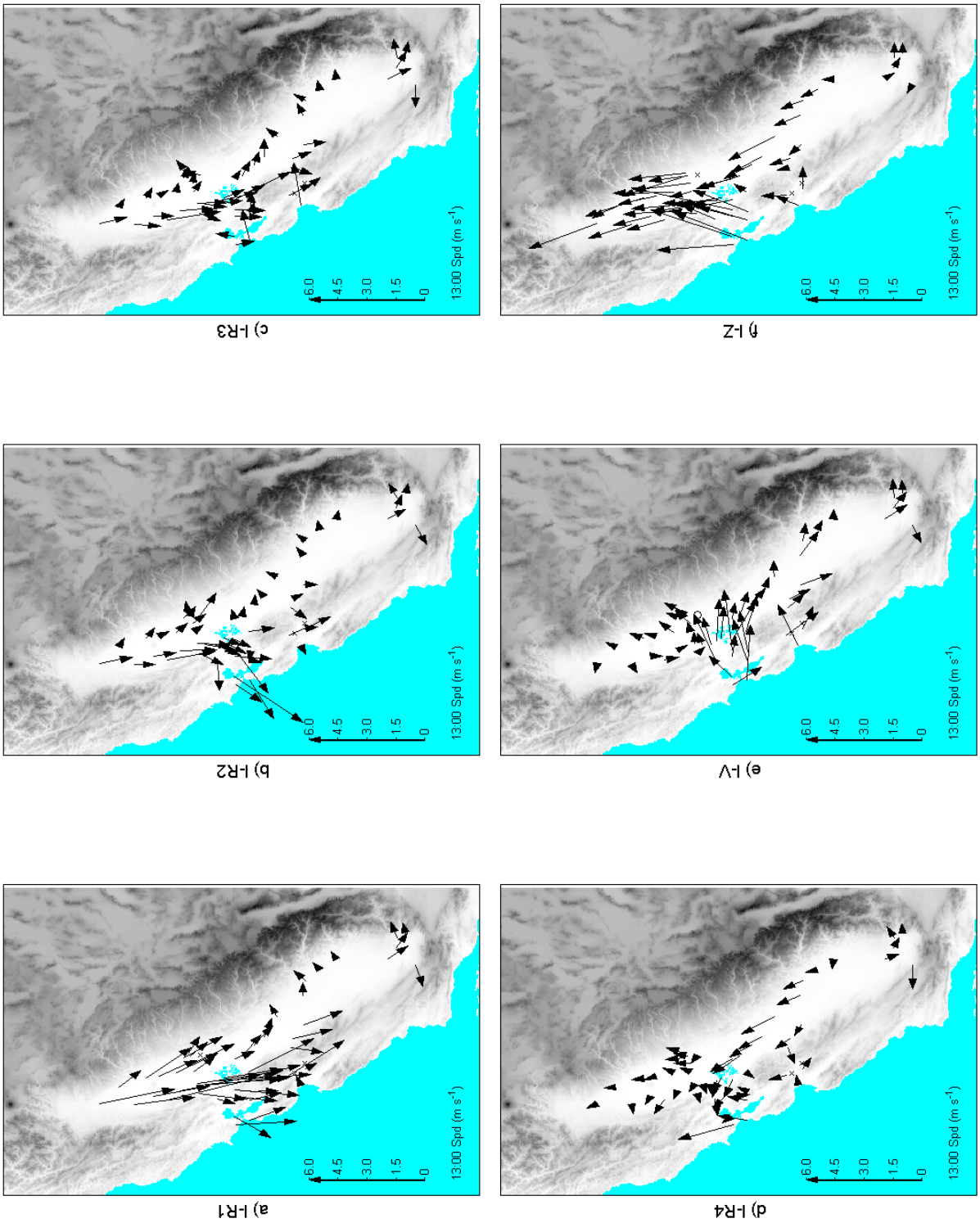

Figure 9. Mean 1300 PST surface wind fields for 6 winter clusters, shown for SFBA and Central Valley monitors. Length of arrow is proportional to mean wind speed, as indicated on scale. Arrows point along wind direction, with tail at weather station position.

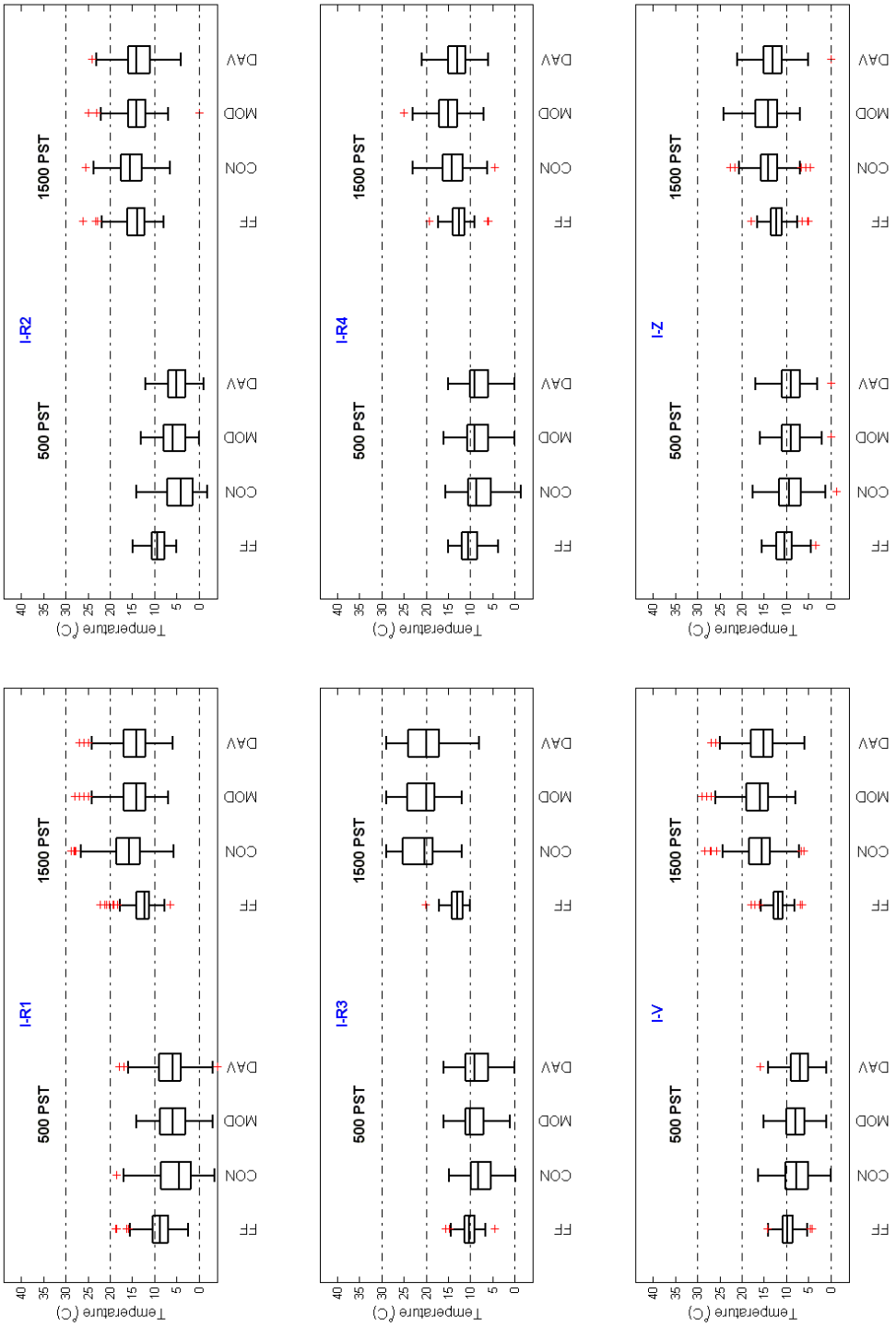

Figure 10. Overnight (0500 PST) and afternoon (1500 PST) temperatures at 4 sites for 6 winter clusters. FF is Fort Funstion, CON is Concord, MOD is Modesto, and DAV is Davis. Boxes indicate the 25-75 percentile range with the horizontal line inside at median. Maximum whisker length is 1.5 times the interquartile range. Outliers indicated using plus signs.

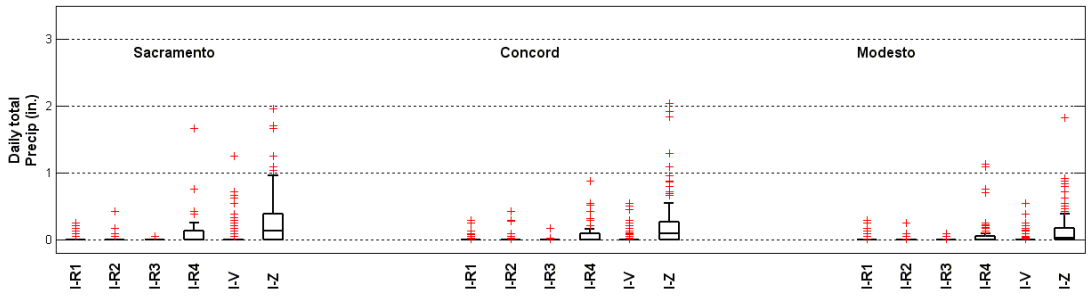

Figure 11. Daily precipitation at 3 sites for 6 winter clusters. Boxplots explained in Figure 10 caption.

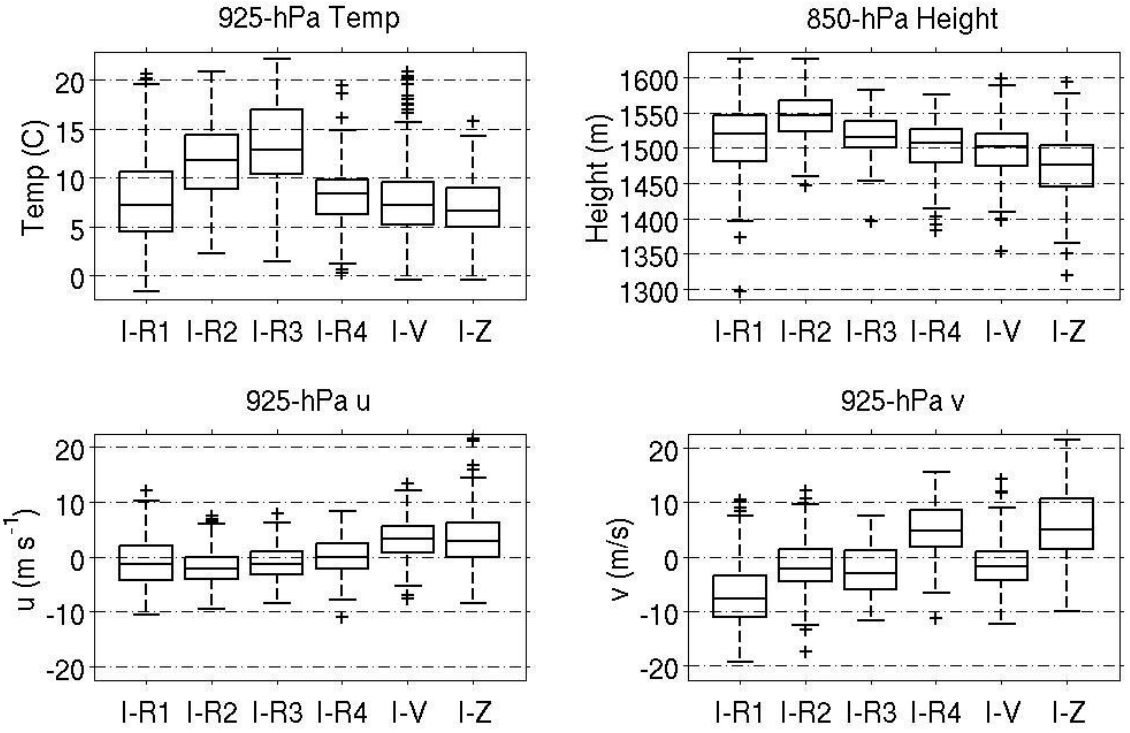

Figure 12. Distribution of 0400 PST Oakland sounding measurements for 6 winter clusters: 925-hPa temperature and *u* and *v* wind components; 850-hPa geopotential height. Boxplots explained in Figure 10 caption.

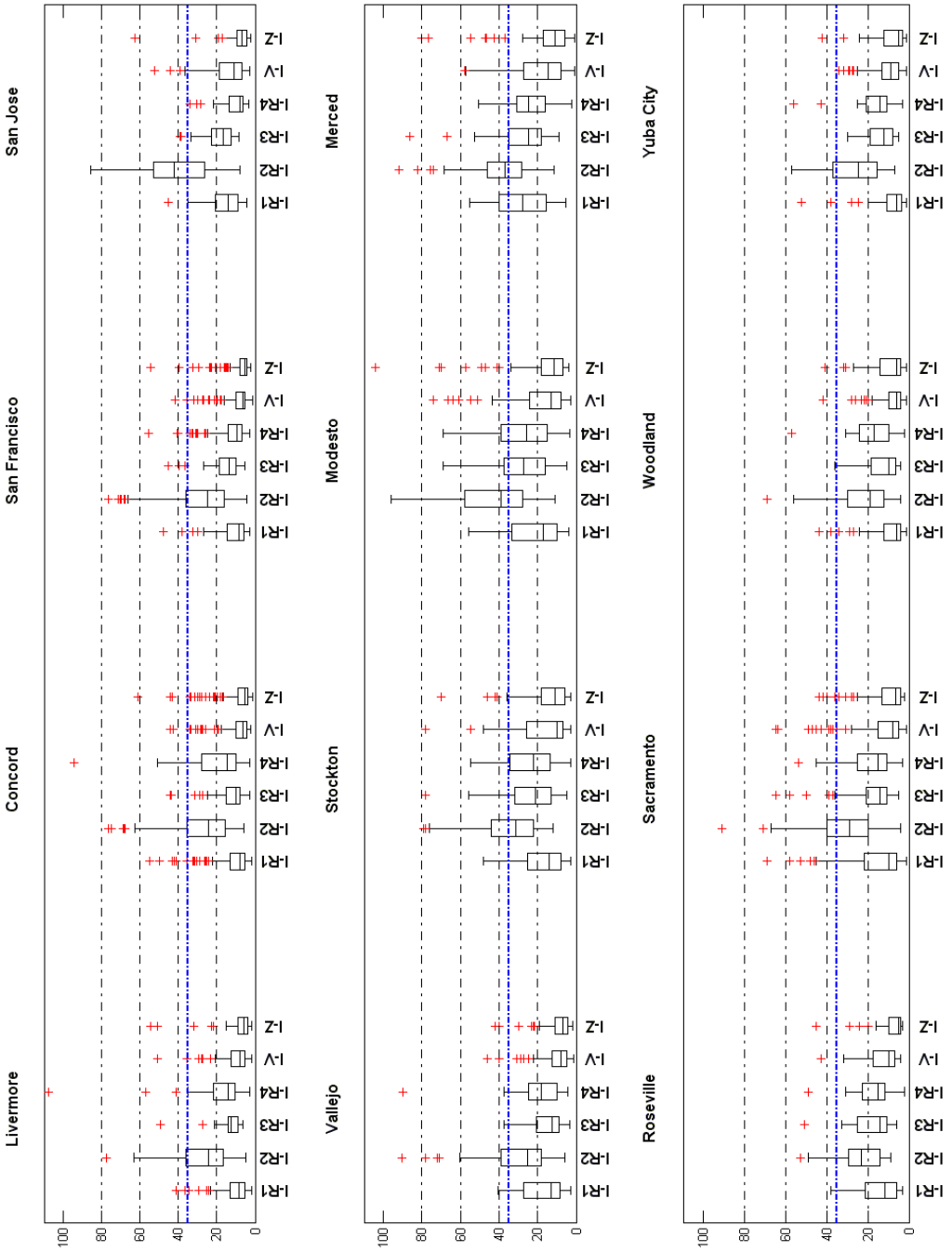

Figure 13. 24-hr total $PM_{2.5}$ levels for 6 winter clusters. Solid horizontal line is exceedance threshold. Boxplots explained in Figure 10 caption.

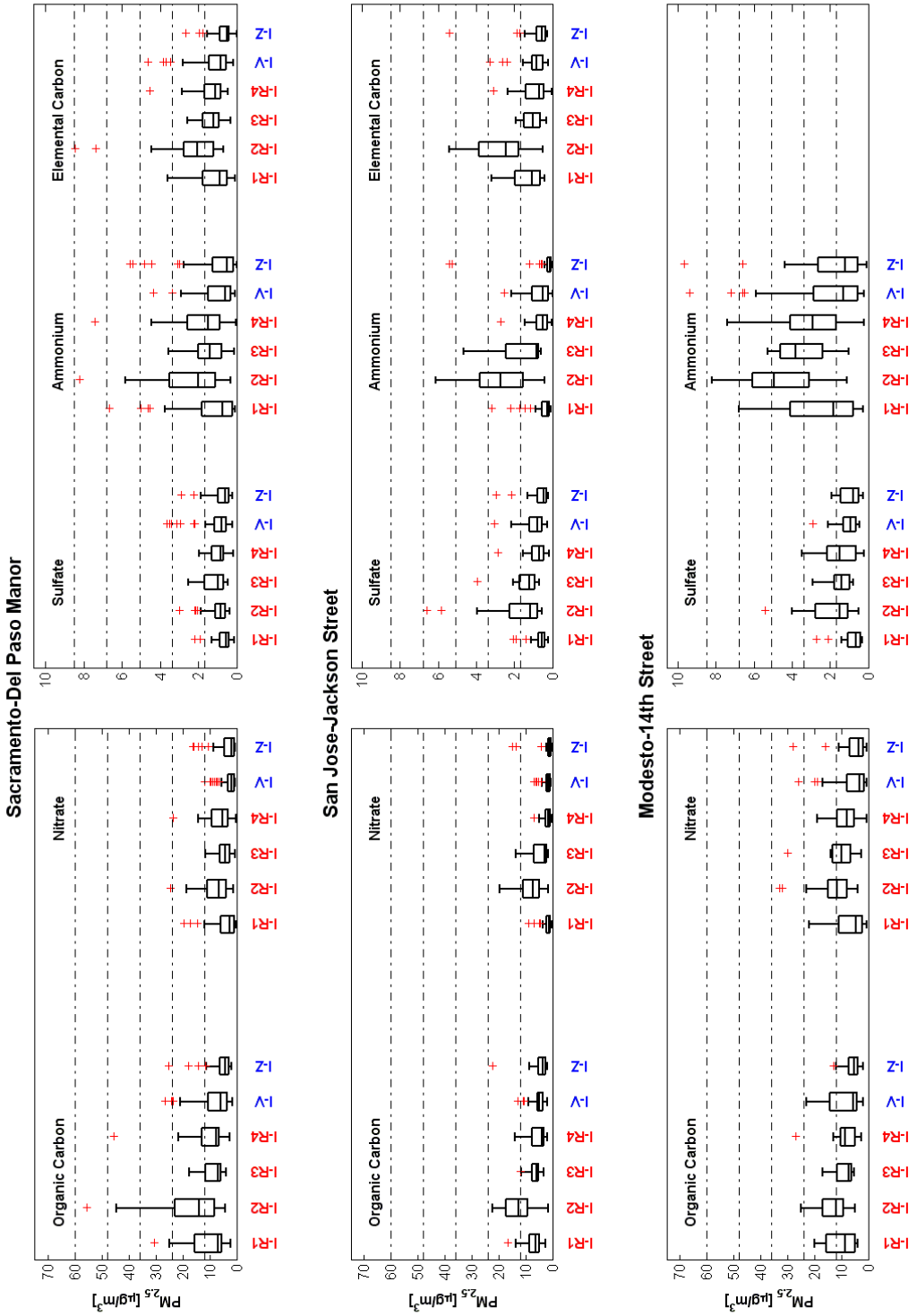

Figure 14. 24-hr levels for dominant $PM_{2.5}$ components for 6 winter clusters. Boxplots explained in Figure 10 caption.

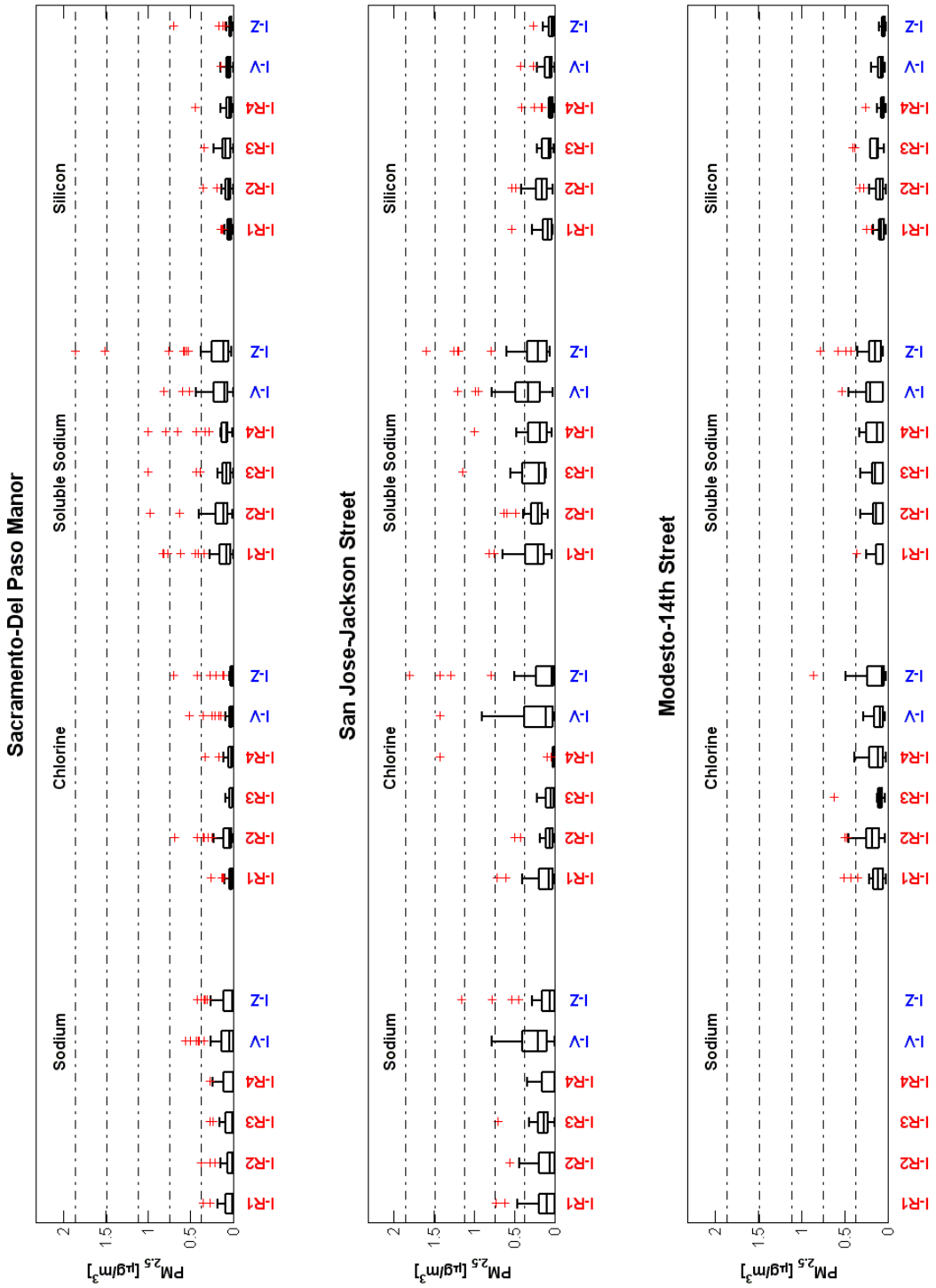

Figure 15. 24-hr levels for trace $PM_{2.5}$ components for 6 winter clusters. Boxplots explained in Figure 10 caption.

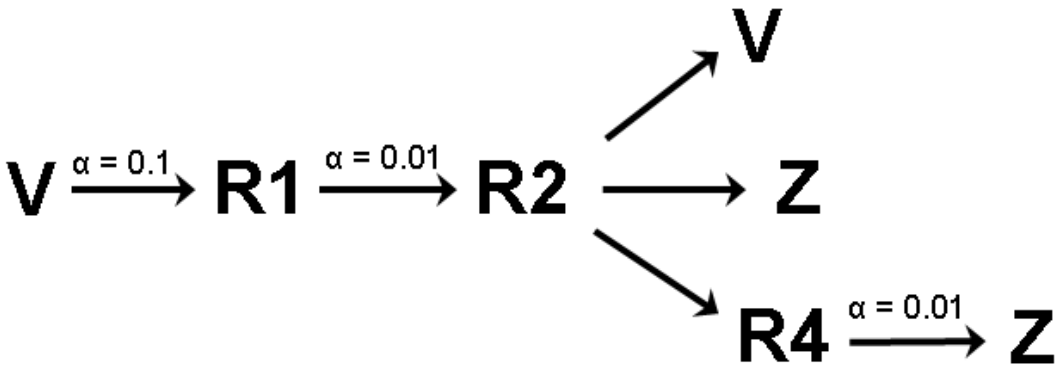

Figure 16. Diagram indicating favored atmospheric transitions among 6 winter clusters. The diagram indicates 3 idealized atmospheric evolutions under which SFBA $PM_{2.5}$ episodes occur. Level of significance (α) indicated for the highly favored transitions.

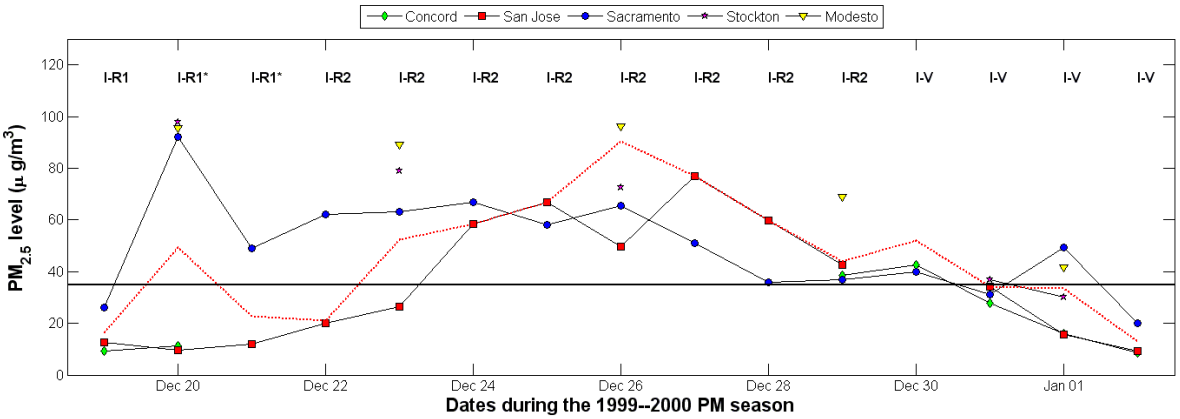

Figure 17. Gradually terminating $PM_{2.5}$ episode developing under idealized I-R1→I-R2→I-V sequence (Figure 16 upper path). 24-hr $PM_{2.5}$ levels shown for key stations in the SFBA, around Sacramento, and in northern SJV. Horizontal line at exceedance threshold. Cluster labels shown across top.

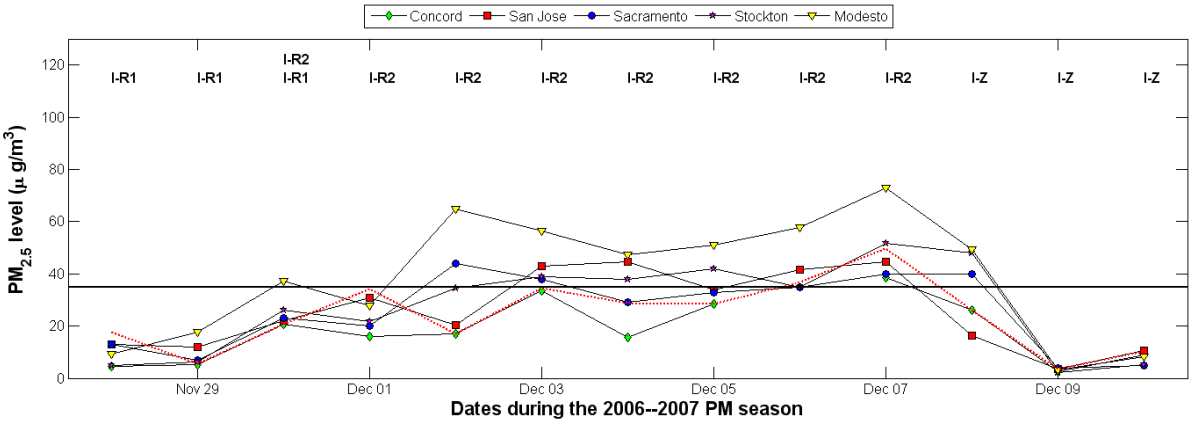

Figure 18. Rapidly terminating $PM_{2.5}$ episode developing under idealized I-R1→I-R2→I-Z sequence (Figure 16 middle path). 24-hr $PM_{2.5}$ levels shown for key stations in the SFBA, around Sacramento, and in northern SJV. Horizontal line at exceedance threshold. Cluster labels shown across top.

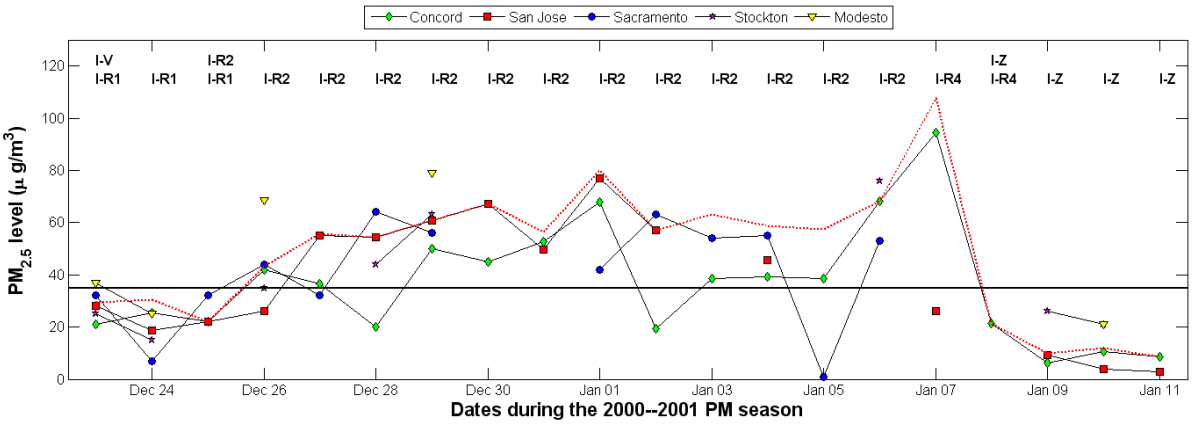

Figure 19. $PM_{2.5}$ episode terminating with transport from SJV developing under idealized I-R1→I-R2→I-R4→I-Z sequence (Figure 16 lower path). 24-hr $PM_{2.5}$ levels shown for key stations in the SFBA, around Sacramento, and in northern SJV. Horizontal line at exceedance threshold. Cluster labels shown across top.

5. Results for summer ozone

5.1 Summer weather patterns

5.1.1 Clustering results and nomenclature

Clustering was performed for 1309 summer (May-October) days with available measurements from the 8-year study period (2000-2007). Seven weather patterns (clusters) were identified having distinct surface air flows, aloft conditions, and ozone spatial distributions. Figure 20 shows the assignment of each day of the study period among the seven clusters. The clusters usually persisted for 3-5 days when they occurred. This persistence time scale implied significant influences of synoptic (large-scale) circulation patterns to drive the Central California weather. Regional surface conditions usually evolved gradually over the course of several days in response to day-to-day changes in the large-scale aloft conditions.

Composite weather maps of cluster-averaged 500-hPa pressure level geopotential height (Figure 21) indicated the aloft conditions associated with each cluster. The aloft patterns were used to name the clusters: I-H, I-H/V, I-V/H, I-V, I-Z, I-R, and I-V/R. The leading "I-" in each cluster name refers to the "inter-regional" nature of the surface flow patterns and distinguishes the results of this study with those obtained in a different but related study funded by the CCOS (Palazoglu, 2009A). The seven summer weather patterns depicted various combinations of four basic aloft large-scale features that could be present on a given day.

- "H" represented an anticyclonic system usually associated with cell of "high pressure" originating over Mojave Desert and/or the Four Corners region.
- "R" represented a strongly anticyclonic system usually associated with a "ridge" of high pressure originating over the Pacific Ocean and migrating eastward toward and over the continent. R was generally more strongly anticyclonic than H.
- "V" represented a cyclonic trough of low pressure usually over the Pacific coastline of California.
- "Z" represented a strongly cyclonic system usually associated with a migrating low pressure cell (storm) at variable position. Z was generally more strongly cyclonic than V. This feature's name was derived from the mean "zonal" (westerly) aloft flow. The cluster composite for Z (Figure 21) was, however, a mathematical artifact. It resulted from averaging pressure fields across days which exhibited low pressure centers at different locations.

The synoptic features and numbers and percentages of SFBA ozone exceedances accounted for by each weather pattern are listed in Table 6. More strongly anticyclonic weather patterns exhibited decreased dispersion and increased conduciveness for

ozone buildup.[2] I-H and I-R were purely anticyclonic and generally produced the highest SFBA ozone levels. More strongly cyclonic weather patterns exhibited increased dispersion and decreased conduciveness for ozone buildup. I-Z and I-V were purely cyclonic and generally inhibited ozone buildup to the exceedance level (85 ppb for 8-hr ozone level). The remaining patterns were hybrids that simultaneously exhibited anticyclonic and cyclonic influences. The first character of a hybrid cluster's name (excluding the leading "I-") reflects the dominant influence. The second letter, appearing after the slash ("/"), reflects the weaker influence. I-H/V and I-V/H were similar weather patterns involving both H-type and V-type aloft features. I-H/V was predominately anticyclonic, whereas I-V/H was predominately cyclonic. I-H/V ozone levels were somewhat lower than for I-H in the SFBA; however, I-H/V had a similar exceedance potential as for I-H. The final pattern, I-V/R, had a moderately cyclonic influence and was far less anticyclonic in nature than I-R.

Figure 22 shows the seasonal distribution of the weather patterns. Episodic patterns I-H and I-H/V occurred mostly from mid-June through late August. The seasonality of these episodic weather patterns with strong onshore high pressure systems together largely accounted for the mid-summer SFBA "ozone season." Mid-summer days that did not experience episode-prone conditions were usually assigned to I-V/H. This pattern was influenced by the semi-permanent summertime onshore high pressure dominant for I-H and I-H/V; however, I-V/H had strong marine ventilation and was not highly likely to produce exceedances. Purely cyclonic patterns I-Z and especially I-V tended to occur mostly before or after the ozone season. Anticyclonic blocking by mid-summer onshore high pressure systems (I-H, I-H/V and I-V/H) inhibited the development into fully cyclonic conditions. Ridging patterns I-R and I-V/R occurred toward the end of the ozone season. I-R accounted for many of the late-summer (September and into October) SFBA exceedances. I-H also occurred during the late-summer and produced exceedances; however, these occurrences usually represented a ridging pattern (I-R) that had migrated over Central California to form an onshore high pressure system.

5.1.2 Surface characteristics

Composite weather maps of cluster-averaged 1000-hPa pressure level geopotential height (Figure 23) indicated the large-scale surface pressure gradients driving the low-level winds through the complex Central California terrain (Figure 24).

I-H, I-H/V, I-V/H, and I-V were similar weather patterns. Each exhibited a cell of high surface pressure west of the SFBA (the North Pacific High) and thermally induced low

[2] Anticyclonic systems are generally associated with sinking (subsiding) and stable air masses. Subsidence generally increases with aloft (850-hPa level) pressure, and stability generally increases with aloft (850-hPa level) temperature. They are also likely to exhibit capping thermal inversions at low altitudes. These characteristics inhibit vertical dispersion, trapping pollutants near the ground level. Anticyclonic systems are also generally associated with weak horizontal large-scale pressure gradients. Shallow, terrain-induced low-level air flows associated with aloft anticyclonic conditions have low wind speeds and little turbulence, inhibiting dispersion by mechanical mixing processes.

surface pressure over the southwestern United States. The strength of the surface thermal low increased with increasing anticyclonic influence (I-H > I-H/V > I-V/H >I-V). Each also exhibited pressure dropping from west to east across much of Central California and nearby offshore locations. Marine flows entered the SFBA and passed through Carquinez Strait into the Central Valley. Patterns with an anticyclonic influence (I-H, I-H/V, and I-V/H) had sufficiently weak large-scale pressure gradients for a localized sea breeze to develop through the Golden Gate and Carquinez Strait. The sea breeze was more prevalent for strongly anticyclonic patterns I-H and I-H/V. Patterns with a cyclonic influence (I-H/V, I-V/H, and I-V) had sufficiently strong North Pacific Highs to channel the large-scale marine winds through Carquinez Strait. The large-scale forcing on the low-level winds increased with increasing cyclonic nature (I-V > I-V/H > I-H/V). The westerly sea breeze and the westerly large-scale flow were superimposed to produce the highest surface wind speeds for I-H/V and I-V/H. I-V winds driven by the large-scale pressure gradient were stronger than for I-H winds that developed locally. The purely localized sea breeze flow for I-H mostly emptied into the SJV without splitting. SV conditions were relatively calm for I-H, except for upslope flows near its rims. The other patterns having large-scale forcing experienced flow splitting at the Delta as the channeled winds were deflected off the Sierra Range. Flows entered both the SV and the SJV for I-H/V, I-V/H, and I-V.

I-R and I-V/R were related weather patterns. I-R usually occurred when Central California was directly under a ridge of aloft high pressure. I-V/R usually occurred when Central California was to the east of an aloft offshore ridge, under its leading (easternmost) edge. Both exhibited surface pressure decreasing from north to south in the Central Valley. The large-scale pressure gradient for I-V/R pushed strong winds into the SV from the north. Friction weakened the winds as they were channeled south along the Central Valley major axis, especially deeper into the SJV. I-R had a relatively weak large-scale pressure gradient. A more localized north-south pressure gradient developed in the Central Valley due to thermally induced low pressure in the SJV. Localized upslope flows were prevalent around the Central Valley rims for I-R. Both ridging patterns exhibited winds emptying from SV into the SJV. Little marine penetration through Carquinez Strait was present for either pattern. (The moderate westerly winds sampled at Mt. Tamalpais and Kregor Peak in the SFBA reflected aloft air flows that did not pass through Carquinez Strait to enter the Central Valley.)

I-Z was unrelated to the other weather patterns that represented Rossby waves associated with the meandering of the jet stream. One major difference was the lack of thermally induced low surface pressure in the SJV. The low surface pressure pushing southward from the Gulf of Alaska may have represented the origin of the stormy I-Z conditions. This expanded arctic low pressure displaced the North Pacific High to produce a large-scale surface pressure gradient decreasing somewhat from south to north. Also, I-Z was markedly different from the other patterns aloft. Strong marine winds entered the SFBA and passed through Carquinez Strait. Unlike the other weather patterns, a portion of the low-level I-Z winds often traversed over the Sierra Range

instead of being deflected deeper into the Central Valley. The deflected I-Z winds mostly emptied into the SV without splitting.

Surface temperature patterns (Figure 25) further characterized the low-level air flow patterns. Central Valley temperatures were highest for I-H and I-H/V. These high inland temperatures reflected intense solar heating under clear-sky mid-summer conditions without deep marine layer intrusion. I-R and I-V/R exhibited the highest coastal temperatures because they had the least marine layer intrusion. Inland temperatures were somewhat lower than for I-H and I-H/V because the R-type patterns occurred frequently during late summer and early fall months. I-V/H and I-Z had strong marine layer intrusion. SFBA temperatures were relatively low, and Central Valley temperatures were moderate. I-V had the deepest marine layer intrusion, resulting in the lowest temperatures throughout Central California.

5.1.3 Vertical dispersion characteristics

Vertical dispersion characteristics were inferred using Oakland sounding measurements from the 850-hPa pressure level (Figure 26) in combination with the above findings.

Geopotential heights (pressures) suggested that strongly anticyclonic patterns I-H, I-H/V, and I-R had subsiding air masses. The highest aloft temperatures for I-H and I-H/V suggested strongly stable conditions, likely with a capping thermal inversion. Aloft temperatures for I-R and I-V/H were moderate; however, I-R often occurred outside of the core summer ozone season and temperatures were seasonally cooler. Occurrences of I-R during the hotter months were likely to exhibit strong stability and capping inversions. Cyclonic patterns I-V/H, I-V, and I-V/R had 850-hPa temperatures on average around 5 degree C cooler than the strongly anticyclonic patterns.

Aloft wind speeds for I-H and I-H/V were low, confirming the absence of large-scale aloft motions. Moreover, surface wind speeds (see Figure 24) were considerably higher than for the aloft winds. This decrease in wind speed with altitude evidenced the decoupling of the shallow, locally generated flows from the aloft air mass. Aloft speeds for I-R were moderate despite little large-scale surface pressure gradient. This apparent discrepancy occurred because I-R was a transient weather pattern. Frictional effects caused an immediate stagnation of the surface winds, whereas inertia maintained moderate speeds aloft. Partially anticyclonic I-H/V had moderate aloft wind speeds that were comparable to the surface winds. The nearly constant speed in the vertical dimension suggested that I-H/V low-level flows were moderately deep. I-V, I-V/R, and I-Z had wind speeds decreasing with altitude, indicating very deep flow patterns affected by surface friction.

Vertical profiles in the boundary layer were quite different for I-Z compared to the other clusters. It had considerably lower pressure, lower temperature, and higher speeds aloft than all other patterns. A large-scale wake resulted over Central California as the fast-moving, unstable I-Z air mass impinged on the Coast Range and then the Sierra Range.

The generated turbulence provided coupling between the clean, aloft air mass and the polluted air mass within the sheltered valleys of the complex Central California terrain. Ozone and precursors were rapidly scoured from the surface.

5.2 Inter-regional air quality patterns

5.2.1 Ozone spatial patterns

Figure 27 shows the spatial distribution for cluster-averaged daily maximum 8-hr ozone levels throughout Central California. Table 7 indicates the proportion of exceedance days assigned to each weather pattern at key Central California monitoring locations and within various subregions.

I-H and I-H/V exhibited similar ozone levels throughout the Central Valley that were considerably higher than for the other clusters. Ozone spatial distributions for this pair of episodic weather patterns were distinguished mostly in the SFBA. I-H experienced higher ozone levels throughout the SFBA. Ozone levels for I-H were much higher than for I-H/V in the East Bay where exceedances were likely to occur. This pair of patterns apparently had similar vertical dispersion characteristics. Surface temperatures were also similar, implying comparable levels of biogenic emissions and photolysis reaction rates. The pair was primarily distinguished by horizontal winds, and possibly also by the depths of their relatively shallow flows (not observed). Differences in the surface flows readily explained differences in the SFBA ozone levels. The stronger and possibly deeper flows for I-H/V ventilated the SFBA somewhat more compared to I-H. The weaker marine flows for I-H produced a sharper sea-land ozone gradient as ozone buildup occurred nearer the coast.

The higher Central Valley wind speeds for I-H/V, especially around the Delta, likely provided increased ventilation relative to I-H. This effect is evidenced around Sacramento. I-H produced exceedances to the east (at Folsom) and south (in Sloughhouse and sometimes Elk Grove) of Sacramento. I-H/V, on the other hand, produced exceedances mostly to the east of Sacramento in Folsom. For both anticyclonic weather patterns, exceedances occurred to the east of Sacramento due to shallow, daytime upslope flows extending from the Sierra slopes over the Sacramento source area. Sacramento area emissions were transported eastward. South of Sacramento, ozone buildup was controlled by marine ventilation through the Delta. The increased marine flows through the Delta for I-H/V relative to I-H pushed Sacramento area emissions north and east. Exceedance potential was reduced to the south of Sacramento for I-H/V. Additionally, it may have been possible for the increased marine flows for I-H/V relative to I-H to have transported pollutants deeper into the SV. I-H and I-H/V surface flows were similar in the SJV, resulting in a similar ozone spatial distribution.

I-R and I-V/R exhibited the highest ozone levels for the coastal locations around the SFBA. The SFBA emissions were not adequately dispersed or transported away from

their sources and ozone formed locally. I-R additionally had relatively high ozone levels in the South SFBA, accounting for most exceedances there, and also in the East SFBA. The increased SFBA ozone levels for I-R over I-V/R were attributed mainly to decreased vertical dispersion under the more strongly anticyclonic conditions. I-R average ozone levels were lower than for the episodic H-type weather patterns (I-H and I-H/V) in the Central Valley. The relatively lower ozone levels could have reflected reduced transport, but they also could have reflected the seasonality of I-R to frequently occur in October. I-R produced exceedances mostly south and east of Sacramento. Sloughhouse exceedances resulted from the lack of marine flows through the Delta, whereas Folsom exceedances resulted from upslope flows toward the Sierra. I-V/R had considerably lower Central Valley ozone levels than I-R, especially around Sacramento. Strong winds for I-V/R ventilated the SV, but may have transported pollutants southward into the SJV as well as westward into the SFBA. I-V/R exhibited high winds along the SJV major axis; however, SJV ozone levels were moderate. The moderate SJV ozone levels for I-V/R may have involved transported pollutants and/or may have resulted from local emissions due to limited vertical dispersion.

I-V/H exhibited moderate ozone levels throughout Central California. High surface winds and moderate vertical dispersion resulted in moderate ozone levels.

I-V and I-Z exhibited relatively low ozone levels throughout Central California. Strong, deep, turbulent flows and adequate vertical dispersion for these cyclonic weather patterns ventilated Central California of regionally accumulated pollutants. One exception is the Central SJV ozone levels under I-V. Central SJV ozone levels were generally relatively low, but exceedances did occur on 17% of the I-V days. Likely, these days exhibited Fresno Eddy development during an occurrence of I-V with reduced turbulence. (The eddy required a relatively stable air mass such that the low-level flows could decouple from the aloft winds to produce a low level jet into the SJV.)

5.2.2 Precursor spatial patterns

Figure 28 shows the spatial distribution for cluster-averaged morning (0400-1200 PST) maximum 1-hr NO levels throughout Central California. For any weather pattern, morning NO levels were highest in the SFBA and around Sacramento. This spatial distribution reflected the intensified morning rush hour emissions for these major urban source areas. The ridging patterns (I-R and I-V/R) had the highest morning NO levels. Lack of marine intrusion allowed these precursors to build to similarly high levels in the SFBA. Around Sacramento, morning NO levels were very high under the stagnating I-R conditions. For I-V/R, the strong SV winds likely advected pollutants southward, possibly transporting them into the SJV as well as the SFBA.

I-H had the next-highest morning NO levels, following the ridging patterns. Reduced vertical dispersion was the primary factor for the buildup of fresh morning emissions. The small amount of marine intrusion allowed for SFBA and Sacramento area precursor levels that were much lower than for the ridging patterns. In the SJV, away from the

source of marine ventilation, NO levels for I-H were similar to the ridging patterns. I-H/V and I-V/H had similar NO levels that were considerably lower than for I-H. Marine flows penetrated the Central Valley for these partially ventilated patterns to reduce precursor levels below that of more stagnant I-H. The similar NO levels for I-H/V and I-V/H likely resulted from different atmospheric processes. I-H/V had less vertical dispersion, serving to increase NO levels. But, I-H/V also experienced more ozone titration, serving to decrease NO levels. I-V had somewhat higher morning NO levels than I-H/V and I-V/H in the SFBA but somewhat lower levels in the Central Valley. Winds through the SFBA were much weaker for I-V than for the patterns with an onshore high pressure system (I-H, I-H/V, and I-V/H), and Central Valley air flows were more turbulent. I-V also occurred outside the core ozone season and may have experienced reduced titration.

I-Z had relatively high morning NO levels. This most strongly cyclonic cluster likely had higher than average precursor levels for two main reasons. First, Z was a transient weather pattern, and may have experienced carry over from more conducive weather patterns occurring on previous days. Second, Z occurred mostly outside the ozone season. Ozone levels were the lowest of any weather pattern. Little removal of NO by ozone titration occurred.

Figure 29 shows the spatial distribution for cluster-averaged afternoon (1200-2000 PST) maximum 1-hr NO_2 levels throughout Central California. The ridging patterns (I-R and I-V/R) had the highest afternoon NO_2 levels that were relatively uniform throughout Central California. The elevated levels resulted from decreased vertical dispersion and lack of marine ventilation. SFBA precursor buildup is especially evident, due to the lack of marine flows. NO_2 levels for I-H were lower than for I-R, especially in the SFBA nearest the source of the marine ventilation. I-H/V, I-V/H, and I-V had similar NO_2 levels that likely resulted from different combinations of marine ventilation, ozone titration, and NO_2 photolysis. I-Z had somewhat higher NO_2 levels than I-H/V, I-V/H, and I-V. Precursors may have been carried over for this transient pattern. Also, NO_2 photolysis rates were likely low, especially under cloudy occurrences of I-Z.

5.3 Evolution of ozone episodes

Figure 30 depicts two pathways describing idealized evolutions of weather patterns associated with SFBA ozone episodes. The diagram indicates all transitions that were favored at a high level of confidence.

5.3.1 Episodes under an offshore ridge

The upper pathway of Figure 30 depicts episodes that developed as an offshore, aloft ridge of high pressure swept eastward across the Pacific Ocean and over Central California. I-V/R occurred as the leading (eastern) edge of the offshore ridge approached the California coastline. The clockwise motion under the leading edge of the ridge produced strong northerly winds over Central California and nearby offshore locations. The strong winds entered the SV from its northern end and emptied into the SJV from

the north and occasionally into the SFBA from the east. The north-south pressure gradient and anticyclonic blocking inhibited large-scale marine flows to enter the SFBA from the west. Little marine intrusion and strong Central Valley flows resulted in above average coastal temperatures and moderate inland temperatures. As a result, the sea-land temperature gradient was less sharp than typical for summer. A localized sea breeze did not develop through Carquinez Strait. The lack of marine intrusion allowed SFBA ozone and precursors to accumulate within the SFBA.

I-R occurred as the ridge advanced eastward to be positioned over Central California. At this point, the large-scale pressure gradient vanished and conditions were near-stagnant throughout Central California. Vertical dispersion was severely inhibited due to increased stability, subsidence, and capping inversion strength of the intensely anticyclonic air mass. SFBA ozone levels spiked sharply over a few days as the transient ridge passed over Central California. SFBA ozone exceedances were likely to occur near the late-summer I-V/R→I-R transitions. Such transitions occurring in late October were less likely to result in exceedances due to decreased photochemical activity.

Often during the late summer, episodes were prolonged when I-R→I-H occurred. The large-scale anticyclonic blocking associated with the ridge allowed development of an H-type anticyclone over Central California and the southwestern United States.

Transitions in the opposite direction of the Figure 30 upper path rarely occurred. Ridges of aloft high pressure generally moved west to east for the northern hemisphere middle latitudes.

5.3.2 Episodes under an onshore anticyclone

The lower pathway of Figure 30 depicts episodes that developed under an onshore H-type anticyclone centered over the southwestern United States. This anticyclone was a semi-permanent aloft feature present for most of the summer after sufficient solar heating of the continent occurred. Its spatial extent varied considerably. Patterns I-H or I-H/V occurred when the semi-permanent anticyclone was positioned over Central California and possibly extended over nearby offshore locations. This generally could occur in two ways. First, anticyclonic blocking by an offshore ridge could lead to onshore anticyclonic development. This is the I-R→I-H transition described in section 5.3.1, linking the upper and lower pathways of Figure 30 to result in prolonged and often severe episodes. Second, the onshore semi-permanent anticyclone expanded west and/or north to be over Central California, without any ridge present.

Once the H-type anticyclone was over Central California, the large-scale pressure gradient weakened considerably. A localized sea breeze developed between the relatively cool coastal locations and the hot Delta and SJV. For I-H, the large-scale pressure gradient nearly vanished and the localized sea breeze was the primary surface air flow feature. The sea breeze did not extend far into the moderately hot SV. Except for along the coast, I-H produced the highest ozone levels of any pattern. SFBA

exceedances were most likely in the East Bay and occasionally in the South Bay. I-H→I-H/V represented a slight strengthening of the large-scale pressure gradient as the H-type anticyclonic pattern dissipated in strength somewhat. The slight west-east pressure gradient generated large-scale marine flows that were superimposed on the localized sea breeze, increasing the overall strength of flow into the Central Valley. Flows through Carquinez Strait split into both the SV and the SJV. Marine intrusion for I-H/V was sufficiently strong to ventilate the South Bay. East Bay and Central Valley ozone levels remained high, and their exceedance potentials were similar as for I-H.

The I-H/V→I-V/H transition represented the point at which the east-west large scale pressure gradient over the Pacific Ocean became strong enough to push sufficient winds through Carquinez Strait to ventilate and cool the Central Valley. The reduced sea-land temperature gradient driving the sea breeze was diminished. Central Valley flows resulted mostly from the deflection of westerly winds passing through Carquinez Strait off the Sierra Range. The flow pattern became deeper and vertical dispersion increased relative to I-H/V. Flow splitting occurred in the Delta. Surface winds speeds were high, but vertical dispersion was still moderately limited by the still mostly anticyclonic air mass over Central California. Ozone exceedances did not occur in the SFBA. Exceedances were about 2-3 times less likely to occur in the Central Valley as compared to I-H and I-H/V. The transition I-V/H→I-V represented the point at which the deep westerly marine flow completely displaced the anticyclonic air mass over Central California. This large-scale I-V flow pattern was considerably deep and exhibited a high degree of vertical dispersion. Exceedances were unlikely, except in Central SJV. The Fresno Eddy inhibited dispersion of the fresh Fresno area emissions. They interacted with any carried over ozone and precursors to produce ozone rapidly.

Transitions in the opposite direction of the Figure 30 lower path occurred frequently. They represented a strengthening of the H-type anticyclone and exhibited increasing ozone levels.

5.4 Transport potential for ozone and precursors

The strongly anticyclonic H-type patterns I-H and I-H/V were most likely to exhibit significant transport from the SFBA into the Central Valley. Shallow flows occurred through Carquinez Strait in combination with inhibited vertical dispersion. I-H was likely associated with transport primarily into the SJV. The flow splitting for I-H/V likely provided significant transport into both the SV and the SJV.

I-H had less vertical dispersion and also less marine intrusion than I-V/H. I-H may have transported pollutant mostly in the northern SJV. Because of relatively slow winds, it is unlikely that SFBA morning emissions reached the central SJV on or before ozone exceedances occurred. I-H/V may have transported pollutants deeper into the Central Valley. However, ozone exceedances are rare for this relatively ventilated transport pattern.

The ridging patterns I-R and I-V/R were unlikely to produce transport from the SFBA when they occurred. The lack of flow through Carquinez Strait decoupled the SFBA from the Central Valley. The northerly flows within the Central Valley likely transported significant amounts of pollutants from the Sacramento area into the SJV and SFBA. The remaining, strongly cyclonic patterns were unlikely to exhibit significant transport. I-V/H and I-V exhibited similar surface air flow patterns to I-H/V; however, vertical structure of the lower atmosphere was very different. These ventilated patterns were relatively deep with adequate vertical dispersion. I-Z was the most turbulent pattern. Adequate vertical dispersion was likely to preclude significant transport. Also, the importance of transport may be minimal for I-V and I-Z because they occurred mostly outside the ozone season.

5.5 Case studies

Two case studies of Central California ozone episodes involving different transport characteristics are provided. Each case study depicts one of the idealized evolutions of weather patterns shown in Figure 30.

5.5.1 An episode under an offshore ridge

Figure 31 shows a late-summer episode developing under an offshore ridge. It fits the conceptual model described in section 5.3.1 and is depicted by the upper pathway of Figure 30. Time series for the weather patterns and ozone levels are shown for 20-28 September 2002. The episode followed the I-V/R→I-R→I-H sequence of weather patterns.

The episode developed as an offshore ridge of high pressure approached the California coastline. Ozone levels were relatively low under I-V/R as strong northerly flows entered the SV from the north. Transport from the SV into the SJV may have occurred. Ozone levels began to increase as the ridge moved over Central California and I-R occurred. Conditions became near stagnant, largely decoupling the SFBA, the SJV and the SV. High ozone levels likely resulted mostly from local emissions.

As the transition into I-H occurred, a sea breeze developed through the SFBA, between the Pacific Ocean and the SJV. The SFBA ozone levels decreased immediately in response to this marine flow. Sacramento ozone levels held approximately constant, indicating little impact from the sea breeze extending mostly into the SJV. In the SJV, however, ozone levels increased. Possibly this increase in the SJV ozone levels occurred in part due to transported precursors from the SFBA by the shallow sea breeze.

As the high pressure system dissipated, large-scale marine winds pushed through the SFBA under I-V/H. This transition into mostly ventilated conditions resulted in sharply decreased ozone levels for the SFBA, Sacramento area, and northern SJV. The sharp decrease in ozone levels for the inland locations suggested that the strong marine winds

ventilated the Central Valley. Significant pollutant transport did not appear to occur under these conditions.

5.5.2 An episode under an onshore anticyclone

Figure 32 shows a mid-summer episode developing under an onshore anticyclone. It fits the conceptual model described in section 5.3.2 and is depicted by the lower pathway of Figure 30. Time series for the weather patterns and ozone levels are shown for 7-17 July 2002. The episode followed the I-H→I-H/V→I-V/H sequence of weather patterns.

Initially, clean conditions occurred as strong marine winds entered the SFBA under a coastal trough influence. The semi-permanent onshore anticyclone expanded over Central California as a transition into I-H occurred. The anticyclonic influence blocked large-scale marine winds from entering Central California. A localized sea breeze developed through the SFBA and into the SJV. Transport into the SJV was likely to have occurred. Upon the transition into I-H/V, marine flows into the SV were restored. Sacramento area ozone levels were considerably higher than for other locations, possibly due to a combination of local and transported pollutants. The strong marine flows upon the transition into I-V/H ended the episode.

Table 6. Names, number of days assigned, number of SFBA 8-hr ozone exceedance days, proportion of SFBA 8-hr ozone exceedances accounted for (of 96 total during the study period), and synoptic features for 7 summer clusters.

Cluster Label	# days	Exceedances	% exceedances accounted for	Synoptic feature(s)
I-H	126	30	29	Onshore anticyclone
I-H/V	181	33	32	Onshore anticyclone (dominant) with coastal trough
I-V/H	378	8	8	Coastal trough (dominant) with onshore anticyclone
I-V	275	2	2	Coastal trough
I-Z	115	0	0	Cyclone with inland ridge
I-R	115	24	24	Offshore ridge of high pressure
I-V/R	97	5	5	Offshore ridge of high pressure with coastal trough

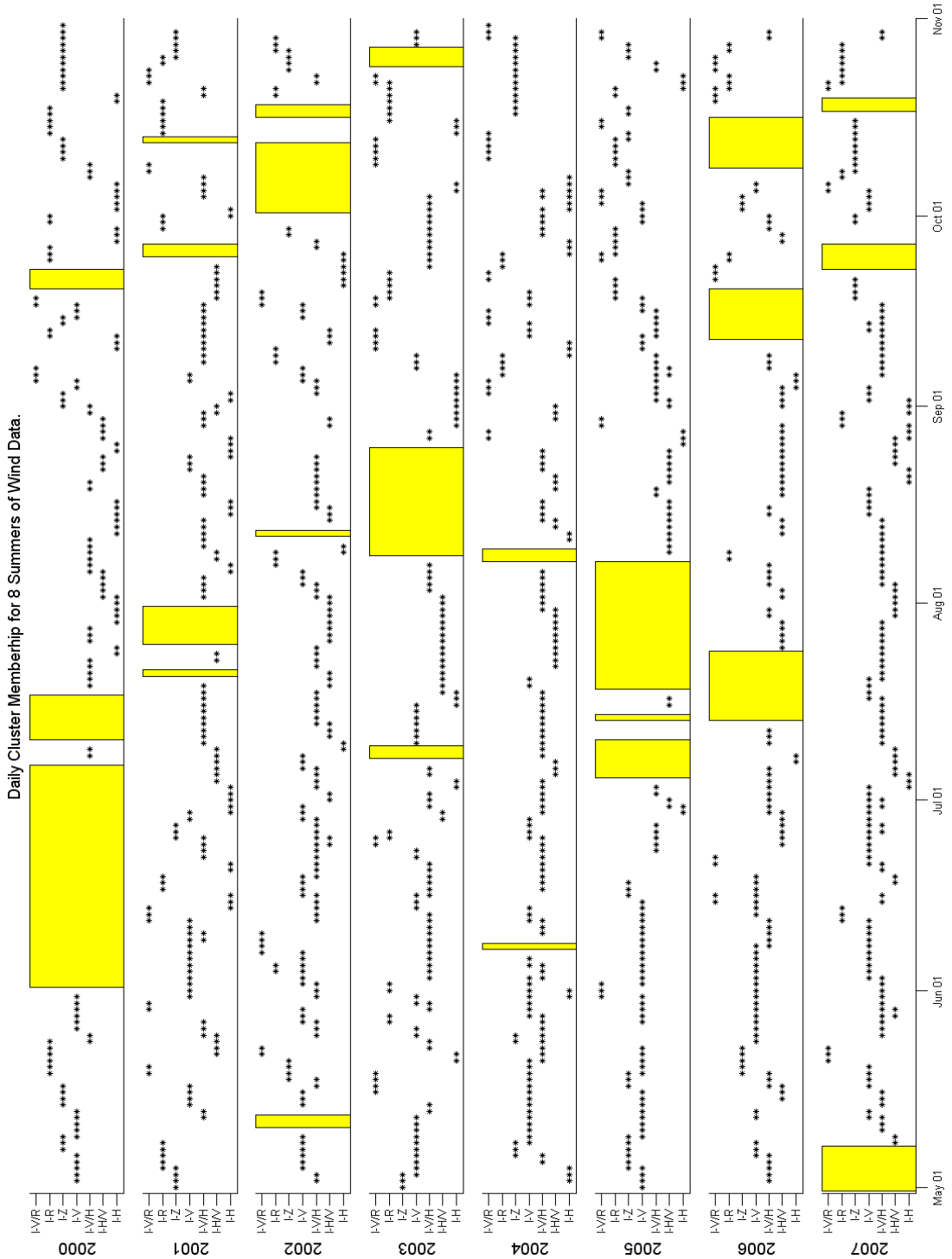

Figure 20. Cluster assignments for 1 May through 31 October of 2000-2007 summer study period. Y-axis position of each marker indicates a cluster assignment for that day. Tick marks (from bottom to top) correspond to clusters I-H, I-H/V, I-V/H, I-V, I-Z, I-R, and I-V/R. Days blocked out in yellow were excluded from the cluster analysis.

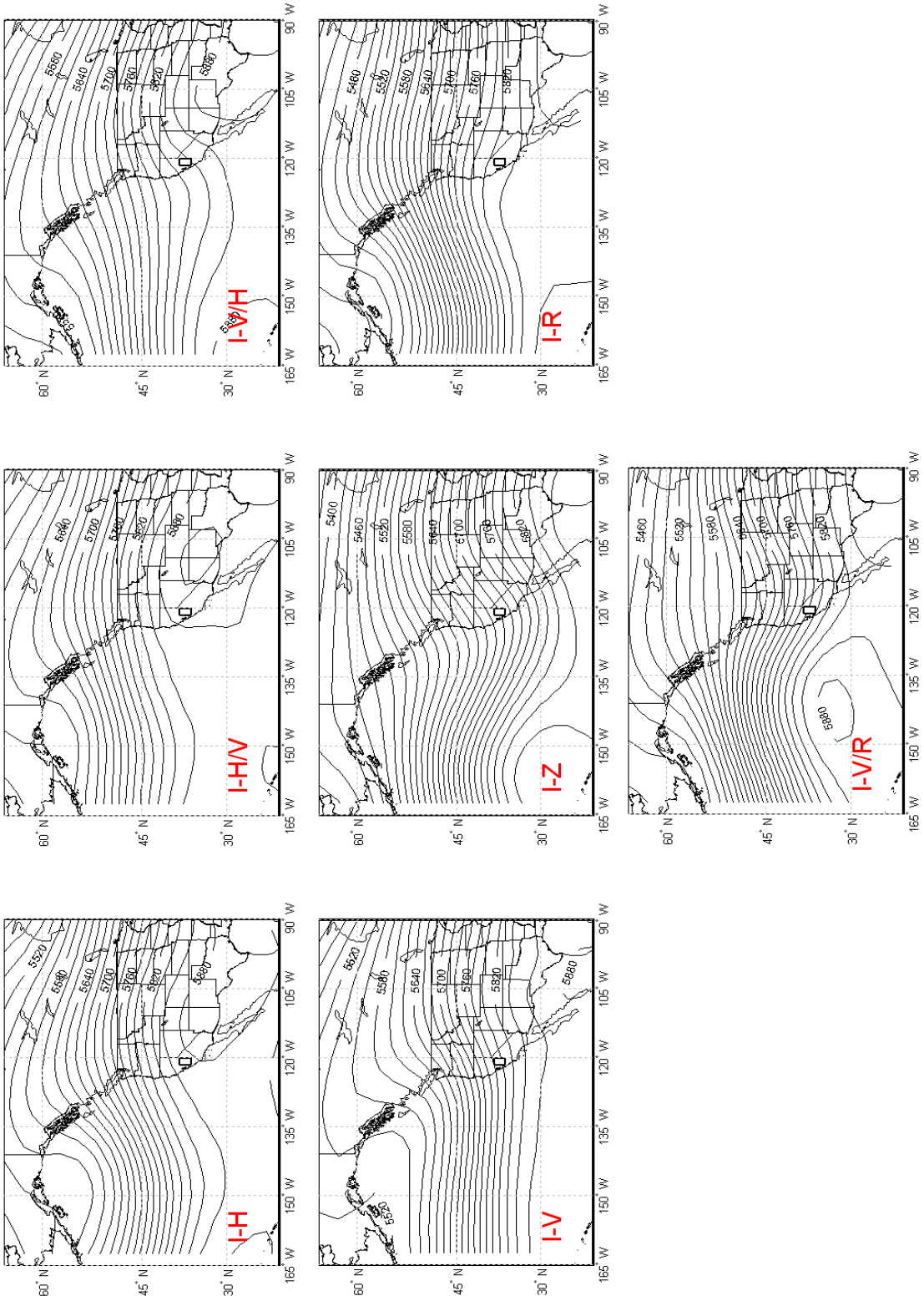

Figure 21. Composite 1800 UTC 500-hPa weather maps for summer clusters, averaged among the days assigned to each cluster. Contours are spaced at 20 m intervals and labeled every 80 m.

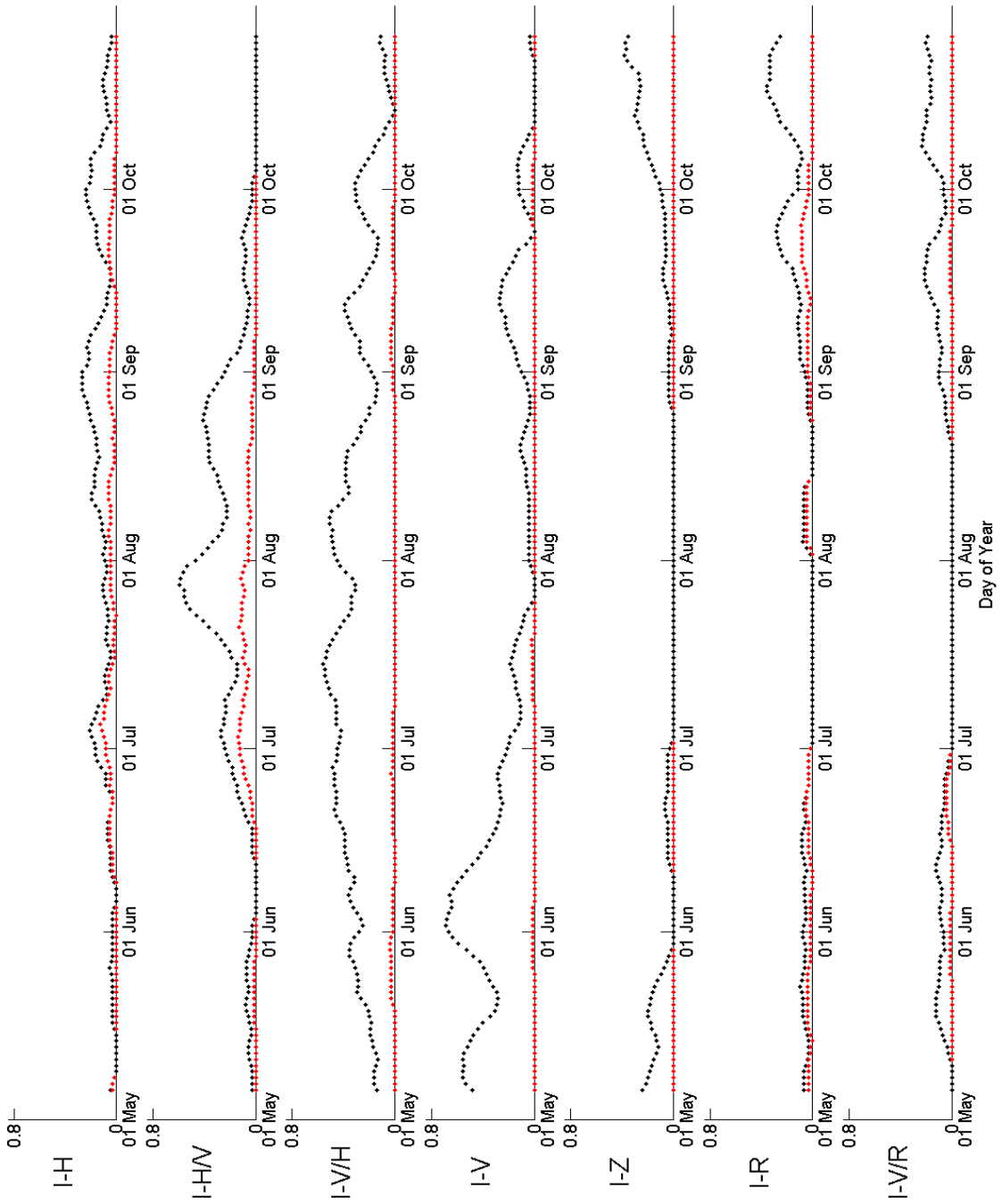

Figure 22. Seasonal distribution for 7 summer clusters. Upper black curves indicate historical frequencies of occurrence for the clusters across the summer season. Lower red curves indicate historical conditional probabilities for the clusters to occur and result in an 8-hr ozone exceedance in the SFBA.

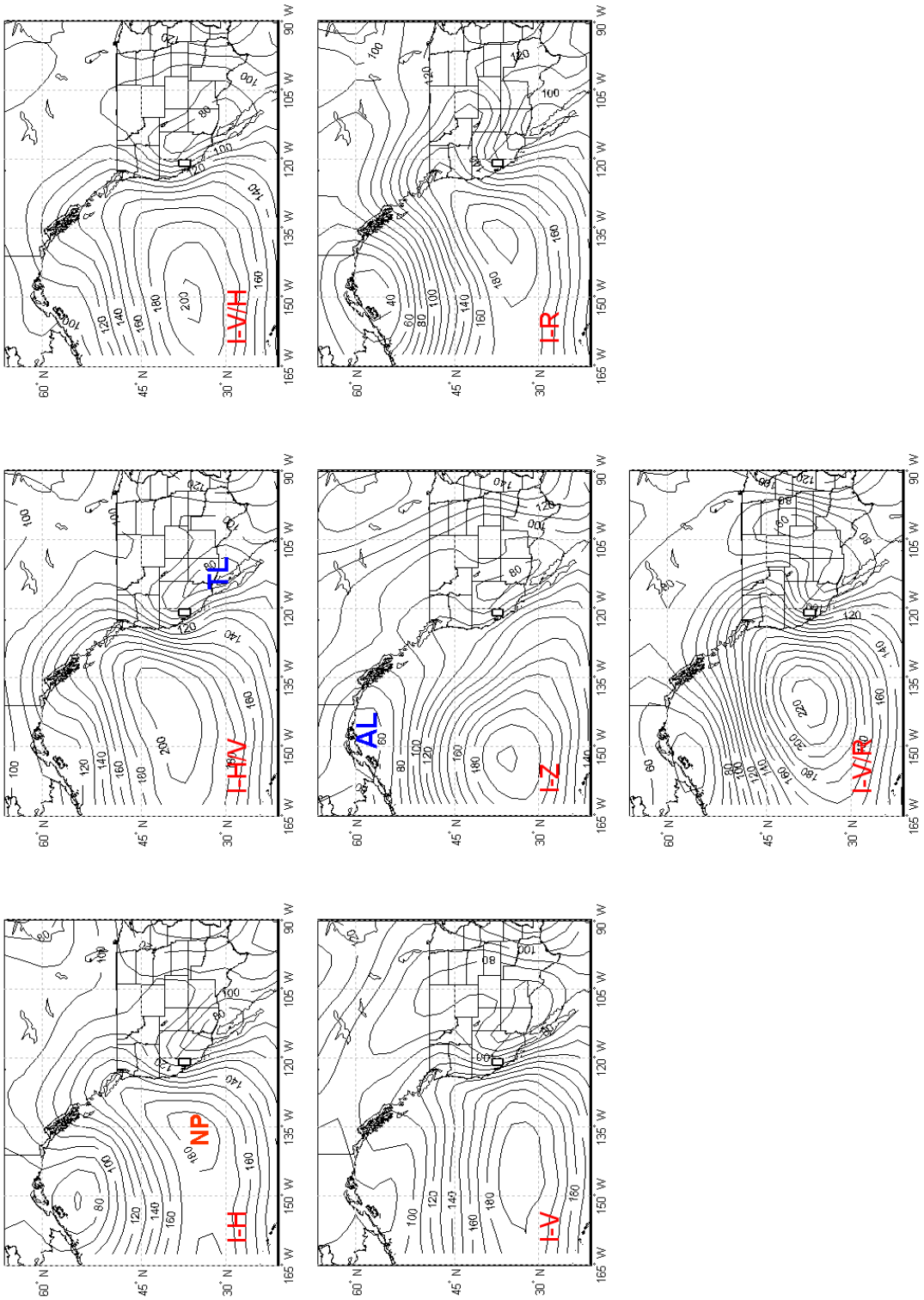

Figure 23. Composite 1800 UTC 1000-hPa weather maps for summer clusters, averaged among the days assigned to each cluster. Contours are spaced at 10 m intervals and labeled every 20 m. “TL”, “NP”, and “AL” indicate positions of thermally induced low pressure, the North Pacific High, and Aleutian low pressure systems, respectively. Each of these features is shown for only a single cluster for clarity.

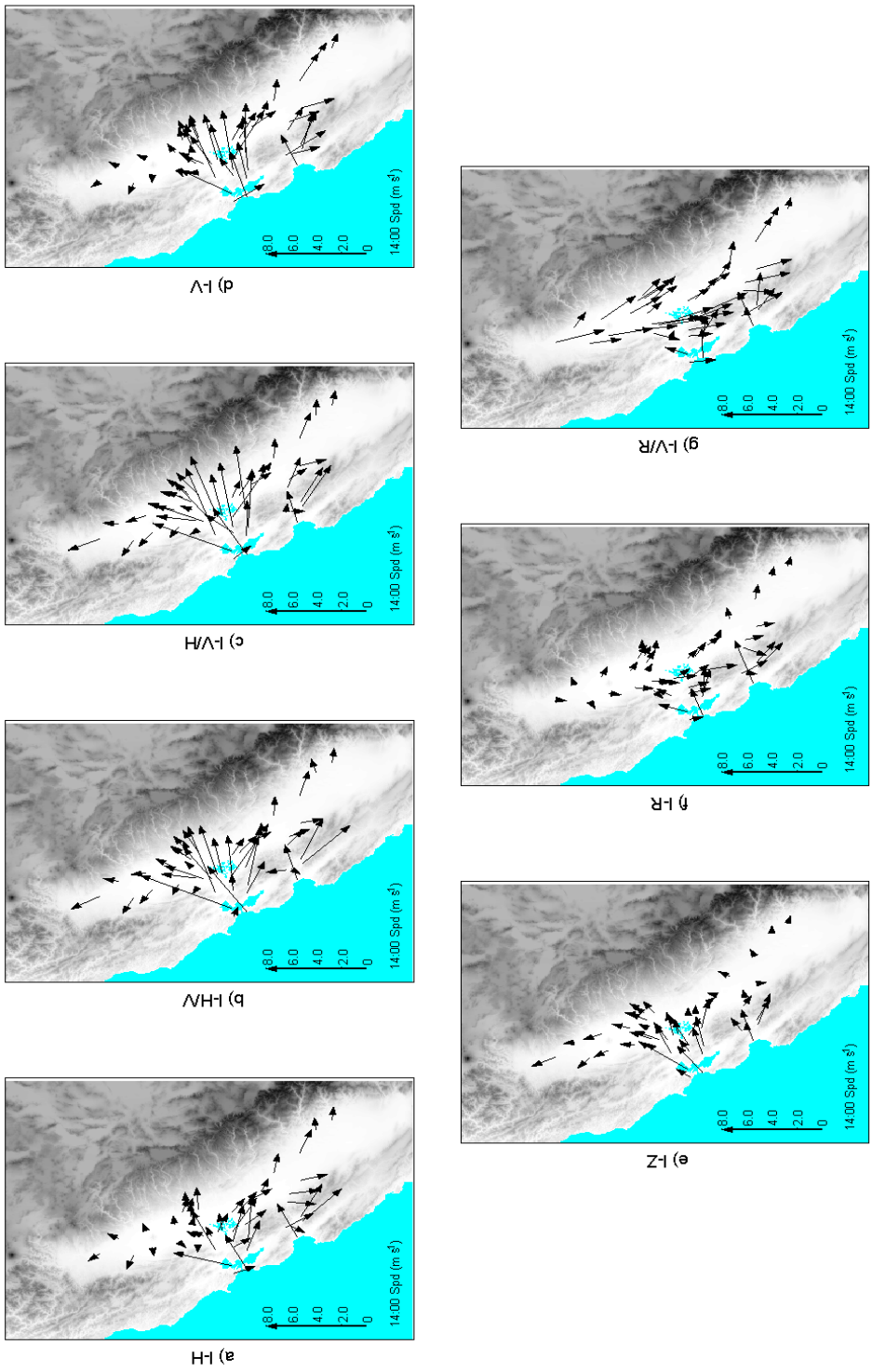

Figure 24. Mean 1400 PST surface wind fields for 7 summer clusters, shown for SFBA and Central Valley monitors. Length of arrow is proportional to mean wind speed, as indicated on scale. Arrows point along wind direction, with tail at weather station position.

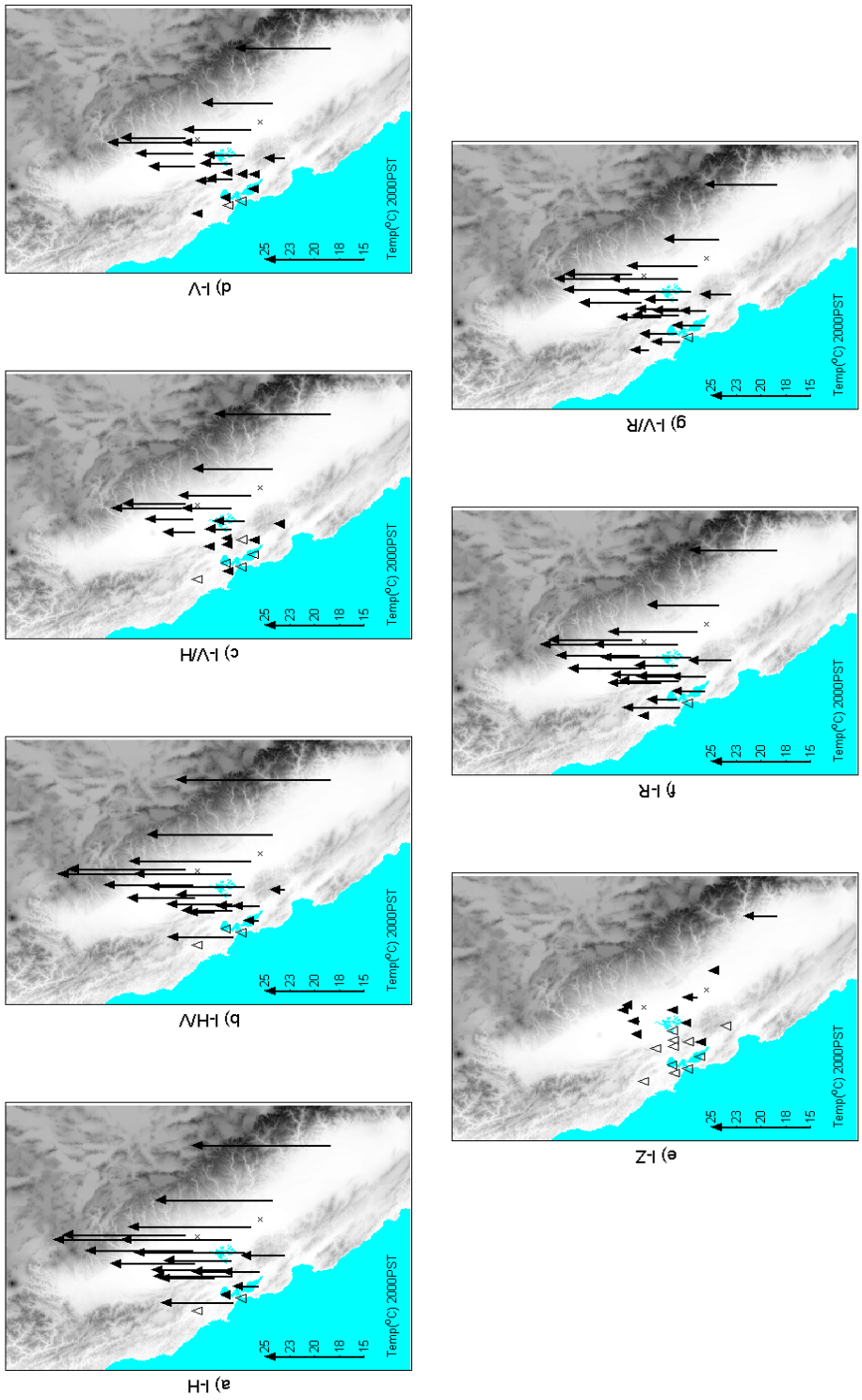

Figure 25. Mean 2000 PST surface temperature fields for 7 summer clusters, shown for SFBA and Central Valley monitors. Height of arrow is proportional to mean temperature, as indicated on scale. Empty arrow heads (triangles) indicate values below scale minimum. Arrow tails at weather station positions.

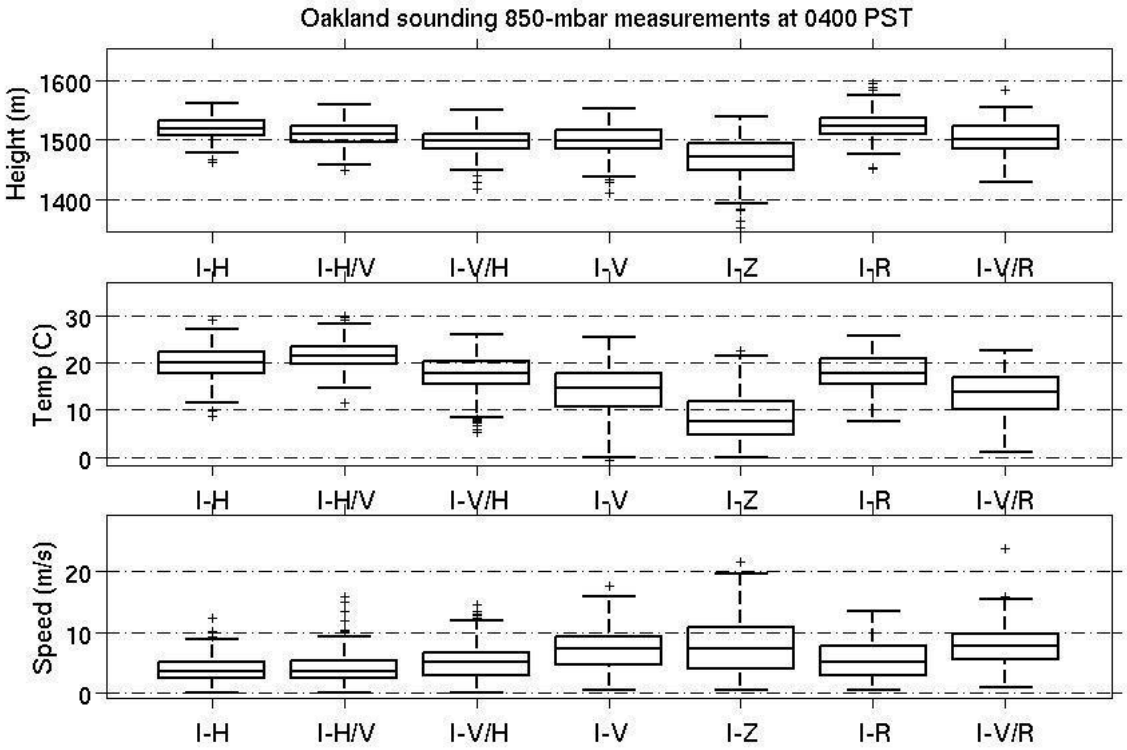

Figure 26. Distribution of 0400 PST Oakland sounding measurements at 850-hPa pressure level for 7 summer clusters: geopotential height, temperature, and wind speed. Boxplots explained in Figure 10 caption.

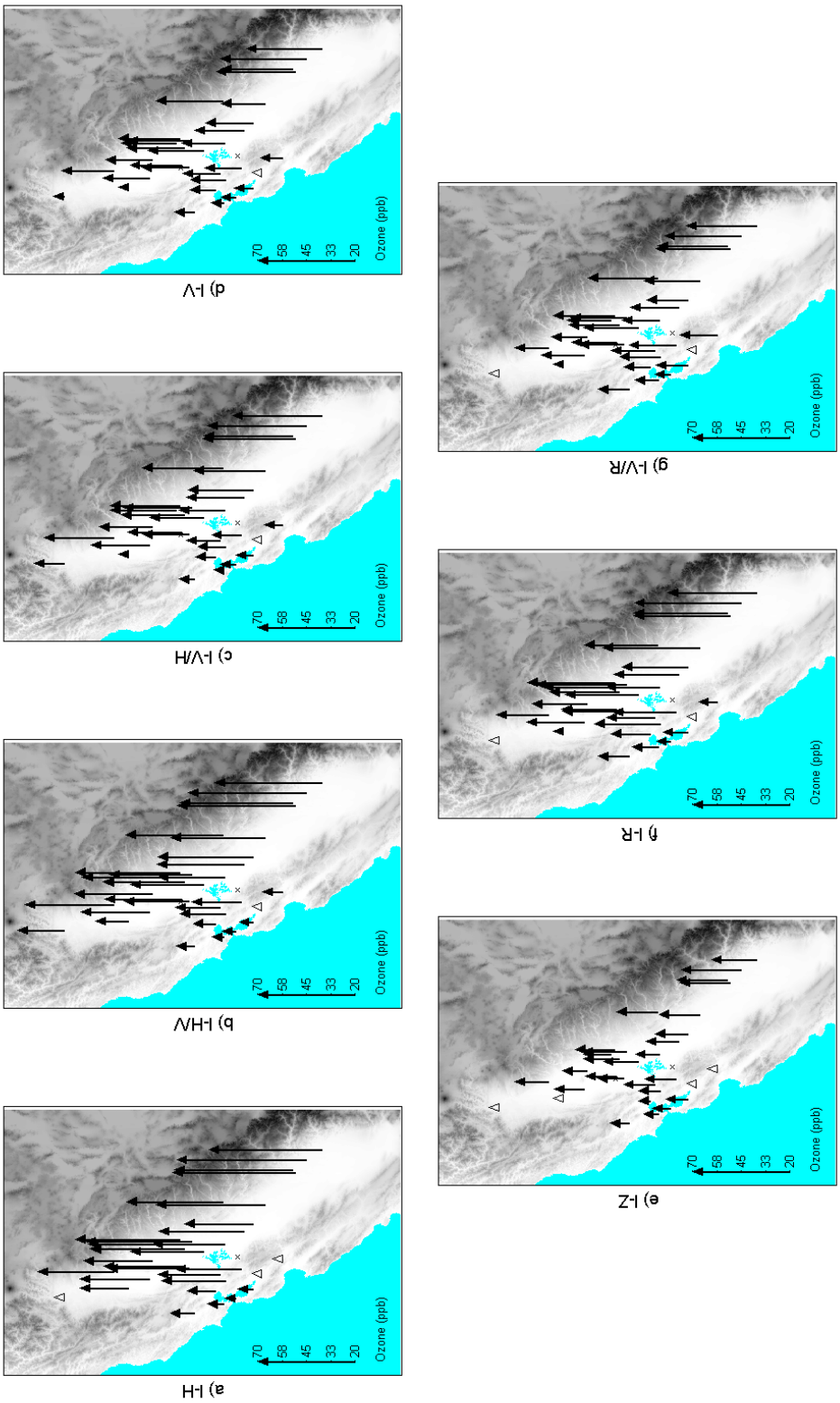

Figure 27. Mean daily maximum 8-hr ozone levels for 7 summer clusters, shown for SFBA and Central Valley monitors. Height of arrow is proportional to mean ozone level, as indicated on scale. Empty arrow heads (triangles) indicate values below scale minimum. Arrow tails at monitoring locations.

Table 7. Fraction of days in each cluster resulting in 8-hr ozone exceedances at individual monitoring locations and totaled for 6 subregions.

Cluster Label	**I-H**	**I-H/V**	**I-V/H**	**I-V**	**I-Z**	**I-R**	**I-V/R**
Number days	126	181	378	115	275	115	97
East Bay	0.14	0.05	0	0	0.01	0.11	0.03
Vallejo	0	0	0	0	0	0	0
Concord	0.10	0.02	0	0	0	0.10	0.02
Livermore	0.14	0.05	0	0	0.01	0.06	0.02
South Bay	0.05	0	0	0	0	0.09	0.03
Gilroy	0.05	0	0	0	0	0.09	0.03
San Jose	0	0	0	0	0	0	0
North SJV	0.55	0.56	0.26	0.03	0.10	0.37	0.19
Stockton	0.10	0.06	0	0	0	0.03	0.01
Modesto	0.21	0.18	0.02	0	0.01	0.10	0.02
Merced	0.53	0.53	0.25	0.03	0.10	0.36	0.18
Turlock	0.28	0.28	0.04	0	0.02	0.19	0.03
Central SJV	0.79	0.84	0.48	0.08	0.29	0.57	0.27
Visalia	0.68	0.55	0.23	0.02	0.13	0.34	0.11
Fresno	0.65	0.67	0.26	0.03	0.13	0.39	0.15
Clovis	0.63	0.64	0.21	0.04	0.06	0.41	0.10
Parlier	0.77	0.72	0.42	0.07	0.25	0.53	0.25
South SacValley	0.56	0.51	0.13	0.01	0.07	0.35	0.10
Sacramento	0.36	0.26	0.05	0	0.03	0.16	0.05
Roseville	0.23	0.24	0.07	0.01	0.01	0.09	0
Elk Grove	0.20	0.07	0.01	0	0.01	0.11	0.01
Folsom	0.47	0.46	0.10	0.01	0.05	0.26	0.04
Sloughhouse	0.45	0.27	0.06	0.01	0.03	0.30	0.06
North SacValley	0.07	0.08	0.02	0.01	0	0.02	0
Chico	0.05	0.06	0.01	0	0	0	0
Colusa	0.05	0.03	0.01	0.01	0	0.02	0
Willows	0.02	0.01	0.01	0	0	0	0
Total (of listed)	0.83	0.91	0.52	0.08	0.31	0.61	0.27

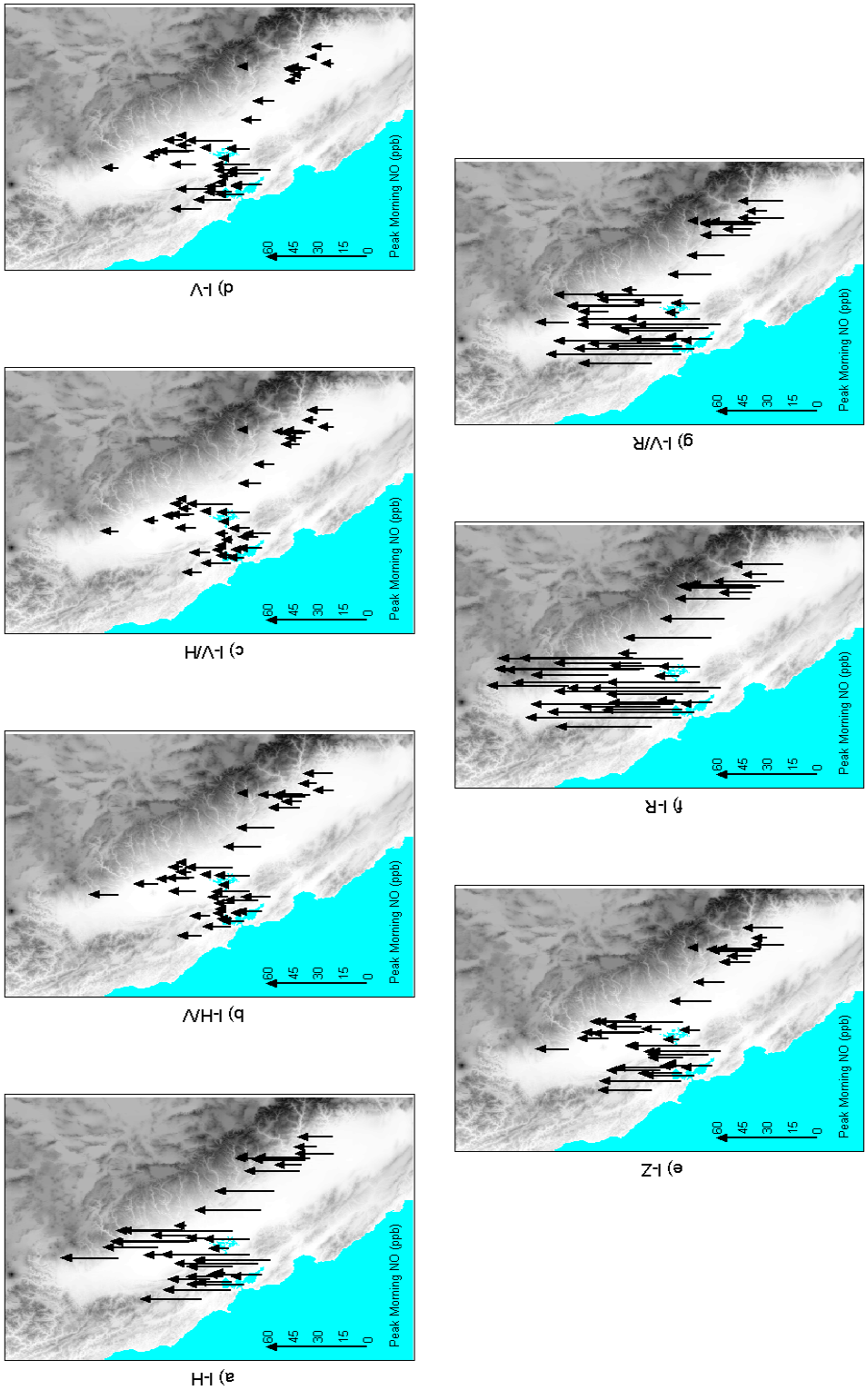

Figure 28. Mean morning hours (0400-1200 PST) maximum 1-hr NO level for 7 summer clusters, shown for SFBA and Central Valley monitors. Height of arrow is proportional to mean NO level, as indicated on scale. Arrow tails at monitoring locations.

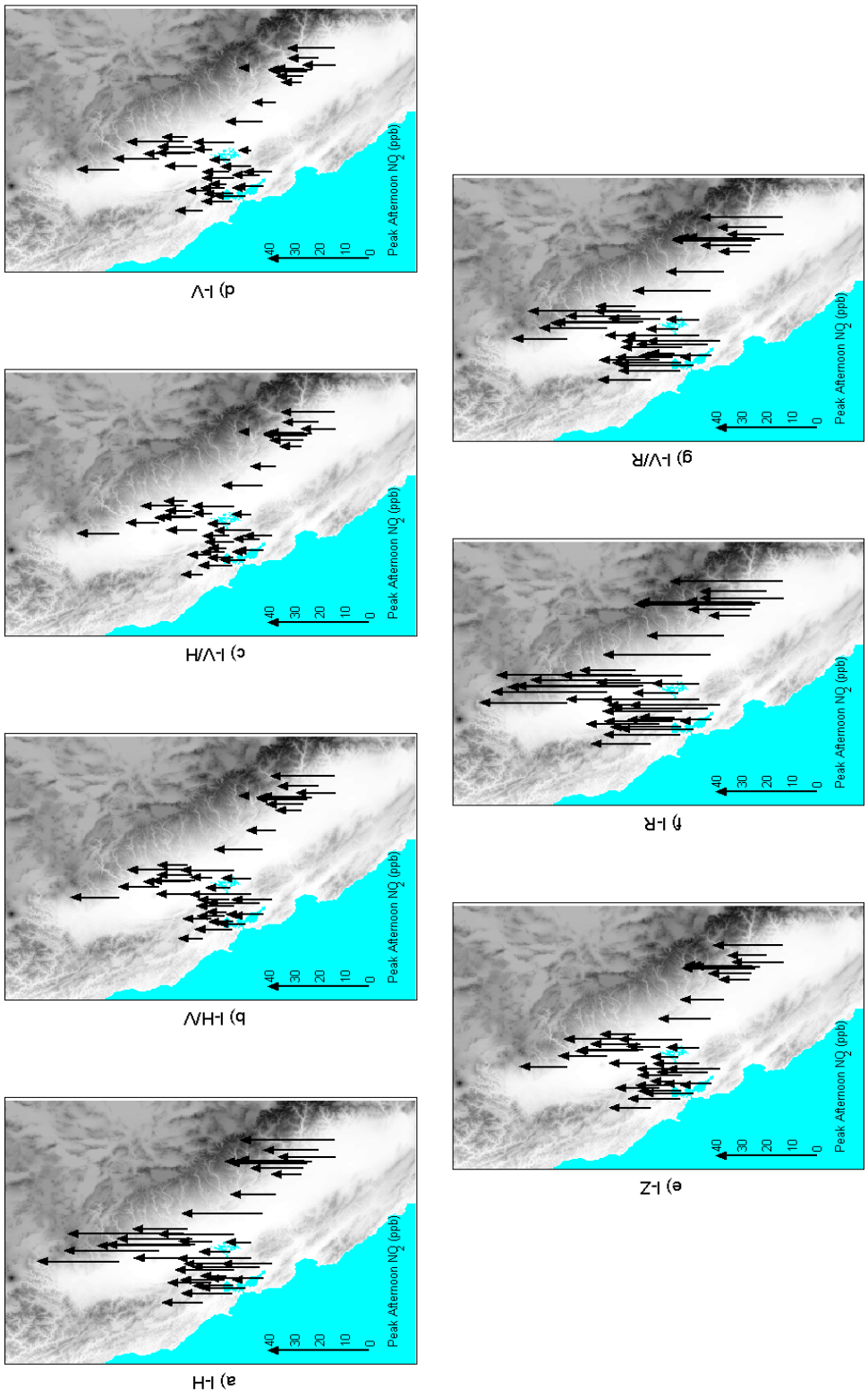

Figure 29. Mean afternoon hours (1200-2000 PST) maximum 1-hr NO_2 level for 7 summer clusters, shown for SFBA and Central Valley monitors. Height of arrow is proportional to mean NO_2 level, as indicated on scale. Arrow tails at monitoring locations.

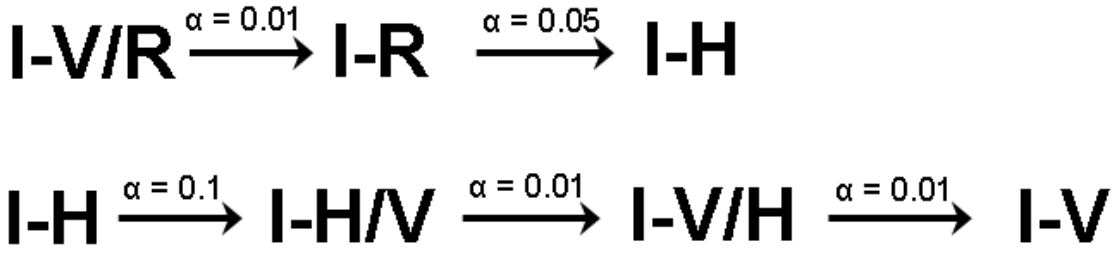

Figure 30. Diagram indicating favored atmospheric transitions among 7 summer clusters. The diagram indicates 2 idealized atmospheric evolutions under which SFBA ozone episodes occur. Level of significance (α) indicated for the highly favored transitions.

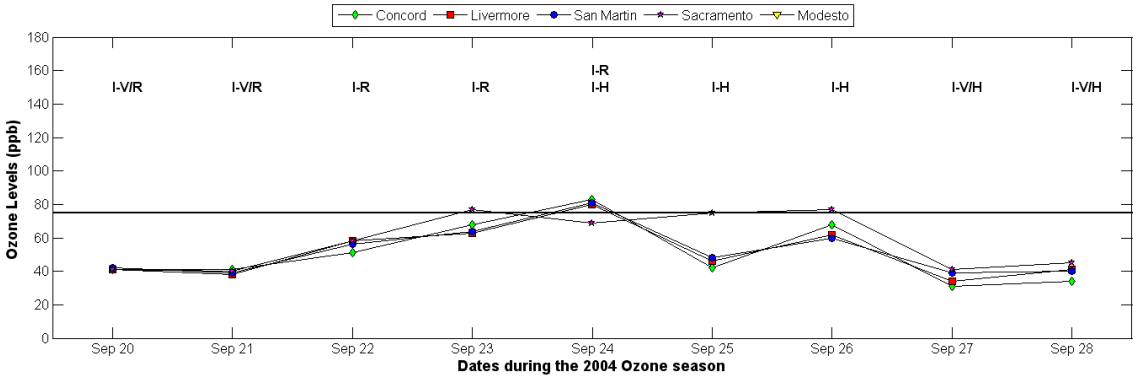

Figure 31. Ozone episode developing under offshore ridge represented by idealized I-V/R→I-R→I-H sequence (Figure 30 upper path). Daily maximum 8-hr ozone levels shown for key stations in the SFBA, around Sacramento, and in northern SJV. Horizontal line at exceedance threshold. Cluster labels shown across top.

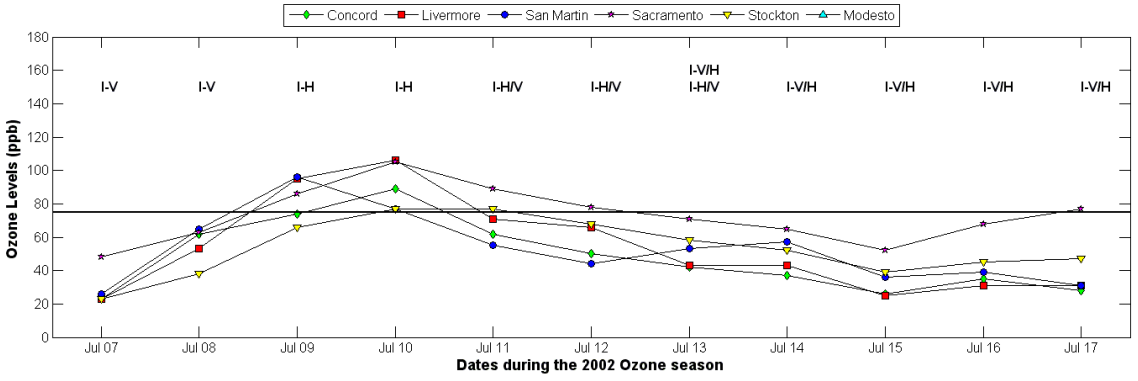

Figure 32. Ozone episode developing under onshore anticyclone represented by idealized I-H→I-H/V→I-V/H sequence (Figure 30 lower path). Daily maximum 8-hr ozone levels shown for key stations in the SFBA, around Sacramento, and in northern SJV. Horizontal line at exceedance threshold. Cluster labels shown across top.

6. Recommendations

6.1 Recommendations for $PM_{2.5}$ transport modeling

We recommend photochemical $PM_{2.5}$ modeling to quantify the transport potential for patterns I-R2 and I-R4. These transport patterns accounted for around 60% and 20% of SFBA 24-hr $PM_{2.5}$ exceedances, respectively. They were likely to have exhibited transport mostly from the Sacramento area and the SJV, respectively. Both were also likely to have exhibited transport into the SFBA from the Delta region. The less frequent I-R4 pattern was generally associated with stronger transport impacts than the more frequent I-R2. For an extreme case (7 January 2001), I-R4 was believed to have provided sufficient transport that would have caused a SFBA 24-hr $PM_{2.5}$ exceedance in the absence of any SFBA emissions.

We recommend that representative, non-extreme instances of I-R2 and I-R4 are modeled for transport evaluation. The extreme 7 January 2001 example verifies the conceptual model established in this current study and also underscores the importance of transport. This episode was, however, not representative and should not be used for air quality planning or policy making purposes.

We also recommend modeling of I-R1 because these conditions lead into most I-R2 type SFBA episodes. Transport may have occurred from the Sacramento area under these conditions and pollutants were accumulated there. Accumulated $PM_{2.5}$ in the SFBA resulting from the I-R1 transport could possibly have been started I-R2 episodes with high background $PM_{2.5}$ levels.

I-R3 occurred outside of the SFBA $PM_{2.5}$ season. Also, the SFBA and Central Valley were largely decoupled under these conditions. Therefore, transport impacts affecting SFBA attainment status were unlikely. Under I-R3, significant $PM_{2.5}$ buildup did occur in the Central Valley. Late-winter transport of the $PM_{2.5}$ that accumulated under I-R3 may impact SFBA attainment status if $PM_{2.5}$ standards are lowered in the future. This potential effect has not been evaluated.

I-V was the only pattern that may have provided significant transport from the SFBA into the Central Valley. Flow splitting occurred around the Delta, such that transport into both the Sacramento area and the SJV was possible. This air flow pattern was, however, deep and turbulent. Significant vertical dispersion inhibited concentrated pollutant advection at low levels. Thus, transport impacts from the SFBA under I-V were likely far smaller in magnitude than transport impacts to the SFBA under I-R2 or I-R4. NO_x transported from the SFBA into the Central Valley under I-V could possibly have contributed to ammonium nitrate formation. It is possible that this ammonium nitrate, partially formed from SFBA NO_x, could have been subsequently transported into the SFBA under other transport patterns such as I-R2. However, this type of transport is expected to be mostly from the northern San Joaquin Valley to the SFBA.

I-Z was unlikely to exhibit transport. These conditions provided substantial vertical dispersion such that concentrated pollutants were generally not transported at low levels.

A recent trend for regulatory agencies is to conduct seasonal $PM_{2.5}$ simulations. Therefore, we recommend selecting multiple core winter periods (at least December and January) exhibiting optimal combinations of the above recommendations. A primary consideration is the selection of winters having non-extreme instances of I-R2 and I-R4 for modeling. In other words, the cluster analysis results presented herein could be used to pool the simulation results across days exhibiting the I-R2 and I-R4 weather patterns to estimate representative transport impacts. Such representative model results would provide the best available technical information as to the degree that SFBA exceedances were dominated by transported versus local $PM_{2.5}$. Modeling could determine the relative amounts of transported $PM_{2.5}$ entering the SFBA through Carquinez Strait, Altamont Pass, and possibly Pacheco Pass. These modeled transport effects could then be confirmed by a tracer field study.

6.2 Recommendations for ozone transport modeling

We recommend photochemical ozone modeling to quantify the transport potential for patterns I-H and I-H/V. Transport impacts may have varied depending on whether the patterns occurred in sequence (i.e. I-H→I-H/V) or not. We recommend transport assessment for episodes involving various combinations of I-H and/or I-H/V.

Modeling may also be performed to confirm the lack of transport from the SFBA during ridging patterns I-R and I-V/R. Estimation of transport impacts between the Sacramento area and the SJV under these ridging conditions may be insightful. These patterns may have represented conditions for which the SJV was impacted mostly by Sacramento area emissions, without significant transport from the SFBA.

We recommend modeling occurrences of I-R followed by either I-H or I-H/V. Transport from the SFBA was unlikely during I-R; however, significant accumulation of ozone and precursors occurred within the SFBA. When followed by a transport-conducive pattern (I-H or I-H/V), the pollution that accumulated in the SFBA under I-R may have been transported into the Central Valley. Thus, modeling of the transport-conducive patterns should be considered for two cases: when preceded by episodic ridging patterns, and when preceded by ventilated conditions. Comparison of transport impacts between these scenarios may provide insight to the split between transported fresh and carried over SFBA emissions. These scenarios differed in both the levels of transported pollutants and also the photochemical ages of the transported air masses. They may have resulted in significantly different impacts on downwind locations.

We recommend limited modeling of strongly cyclonic patterns I-V, I-Z, and I-V/H. Modeling for these weather patterns is simply to confirm their lack of significant

transport. I-V/H likely exhibited more transport than either I-V or I-Z; however, the impacts were likely small.

The above recommendations may best be implemented using seasonal (full-summer) photochemical ozone simulations. Summers should be selected for modeling that contained representative occurrences of the above potential transport scenarios. Modeling of multiple summers would likely increase the sample size to allow more robust estimation of the various transport impacts. Also, multi-year simulations should include years with different overall levels of conduciveness to ozone buildup to account for inter-annual variability in transport impacts.

References

Beaver, S. and Palazoglu, A., 2006. Cluster analysis of hourly wind measurements to reveal synoptic regimes affecting air quality. *Journal of Applied Meteorology and Climatology*, **45**, 1710-1726.

Beaver, S. and Palazoglu, A., 2008. Hourly surface wind monitor consistency checking over an extended observation period. *Environmetrics*, **20**, 399-415.

Beaver, S., Palazoglu, A., and Tanrikulu, S., 2008. Cluster sequencing to analyze synoptic transitions affecting regional ozone. *Journal of Applied Meteorology and Climatology*, **47**, 910-916.

Palazoglu, A., 2009A. Cluster analysis of air quality data for CCOS ozone study. Performed under CCOS contract #06-1CCOS, [Available from California Air Resources Board].

Palazoglu, A., 2009B. Cluster analysis of air quality data for Bay Area PM study. Performed under BAAQMD contract #2007-045, [Available from Bay Area Air Quality Management District].

Schneider, T., 2001. Analysis of incomplete climate data: Estimation of mean values and covariance matrices and imputation of missing values. *J. Climate*, **14**, 853–871.